*Electronic Research Archive*

https://www.aimspress.com/journal/era

ERA, 33(12): 7866–7901.
DOI: 10.3934/era.2025347
Received: 30 October 2025
Revised: 14 December 2025
Accepted: 16 December 2025
Published: 25 December 2025

*Research article*

# Bifurcation analysis of a predator-prey model with cross-diffusion and two delays

**Hongyan Sun[1], Jianzhi Cao[2,*], Pengmiao Hao[2] and Li Ma[2]**

[1] College of Data Science and Software Engineering, Baoding University, Baoding 071000, China
[2] Hebei Key Laboratory of Machine Learning and Computational Intelligence, College of Mathematics and Information Science, Hebei University, Baoding 071002, China

* **Correspondence:** Email: jzcao@hbu.edu.cn.

**Abstract:** In this paper, a predator-prey model with cross-diffusion and two delays is investigated. First, the conditions for local stability and Turing instability of positive steady-state solution are studied separately when the system was without and with diffusion. Second, the existence and the stability of Hopf bifurcation were investigated by computing stability switching curves in the parameter plane with two delays. Moreover, explicit formulas for determining the stability and the direction of the bifurcation periodic solutions were derived using the normal form theory and the center manifold theorem. Finally, the theoretical results were verified by numerical simulations.

**Keywords:** predator-prey system; two delays; cross-diffusion; stability switching curves; Hopf bifurcation

## 1. Introduction

Mathematical modeling is a powerful tool for understanding and predicting the dynamics of complex ecosystems. By abstracting and quantifying key elements in biological processes-such as population growth, interactions, spatial movement, and time delays, it transforms qualitative ecological hypotheses into an analyzable and simulatable quantitative framework [1–4]. Mathematical models enable 'numerical experiments' under controlled conditions, exploring the long-term behavior of systems under various parameters and scenarios, revealing underlying threshold phenomena (e.g., bifurcations), stability transitions, and mechanisms of spatial pattern formation, which are often difficult to obtain through observation or experimentation alone.

As an important part of ecology, population ecology is rich in dynamics and application value. Therefore, scholars have developed a strong interest in population dynamics models. The population dynamics model is a mathematical model that describes the interactions between populations and

the environment, and between populations and populations. The study of these models is of great significance in protecting resources and the environment, maintaining the balance of ecosystems and the rational use of biological resources. It is well known that the relationships among biological populations include four basic relationships: reciprocal symbiosis, parasitism, competition, and predation. Predation relationship plays an important role in the survival and development of the biological community. Hence, the study of the predator-prey dynamics model has also received extensive attention in biomathematics.

In 1926, Lotka [5] and Volterra [6] proposed the most basic and important Lotka-Volterra predator-prey model to describe the dynamic relationship between two populations. Since the establishment of the predator-prey model, the study of this model has been rapidly developed and much research has been carried out on it from different perspectives [7–13]. In 1959, Holling proposed three functional response functions [14], which have promoted the research process of the predator-prey model. It is well known that functional response functions are the key factors to reflect the interaction between predator and prey in the predator-prey model. To describe the characteristics of interactions between populations, many types of functional response functions have been proposed, mostly including Holling type, ratio-dependent type, Hassell-Varley type, Beddington-DeAngelis type, Leslie-Gower type, and Crowley-Martin type. A large amount of research work has been done on these common functional response functions [15–23]. The Leslie-Gower model and its modifications have received great attention, and the modified Leslie-Gower model in [24] is as follows:

$$\begin{cases} \dfrac{\mathrm{d}u}{dt} &= ru(1-\dfrac{u}{K}) - v\psi(u,v), \\ \dfrac{\mathrm{d}v}{dt} &= v(\beta - \dfrac{\gamma v}{u+\alpha}), \end{cases} \tag{1.1}$$

where $u$ and $v$ represent the population density of prey and predators, respectively. $r$, $K$, $\beta$, $\gamma$, and $\alpha$ are positive numbers. $r$ denotes the internal growth rate of the prey. $K$ is the environmental carrying capacity of the prey. The growth rate of the prey is logistic with the carrying capacity $K$ and the intrinsic growth rate $r$. $\psi(u,v)$ represents the functional response function of the predator to the prey. $\beta$ is the internal growth rate of the predator population. $\gamma$ is the maximum per capita reduction rate of predators, and $\alpha$ measures the degree to which the environment protects predators.

In an ecosystem, a species does not always stay in a certain position but migrates due to changes in resources and intra species competition, and diffusion is a common phenomenon. Similarly, population trends are related not only to the current state but also to the state at some time in the past or future, which is known as the delay phenomenon. Therefore, researchers have introduced diffusion or delay into the predator-prey model and conducted numerous studies. For example, Yang [25] investigated the global asymptotic stability and persistence of diffusive predator-prey systems with modified Leslie-Gower functional response. With a deeper study of the predator-prey model, it was found that, by introducing delay in the diffusive system, the system has a richer dynamical behavior. For a detailed example, Yang and Zhang in [24] considered a diffusive predator-prey system with constant prey refuge and delay under Neumann boundary conditions. The local stability and Turing instability of positive equilibrium are investigated, and the property of Hopf bifurcation is determined using the center manifold theorem and the normal form theorem, so the model with delay and diffusion has richer dynamical properties. Therefore, predator-prey models with diffusion and delay have received

widespread attention and research from scholars [26–29]. The types of diffusion can generally be categorized into self-diffusion and cross-diffusion. Moreover, cross diffusion refers to the migration of a population due to the presence of another population [30], and the model with a cross-diffusion term can more accurately reflect the predation relationship between the predator and the prey [31, 32]. Therefore, in this paper, we consider the introduction of cross-diffusion and two delays on the basis of model (1.1).

Although many researchers have focused on predator-prey models with delay or diffusion, studies on Beddington-DeAngelis functional response models that simultaneously incorporate cross-diffusion and two delays (especially production delay and digestion delay) remain relatively limited. Cross-diffusion can more realistically reflect the mutually driven spatial movement between populations, while the two delays can separately capture the feedback delay in prey growth and the physiological delay in predator digestion. However, the spatiotemporal dynamics under the joint effect of both factors, particularly the systematic analysis of delay-induced Hopf bifurcation via stability switching curves in the two-delay planes, has not been fully explored. We aim to fill this gap by systematically analyzing the complex dynamical behaviors of such a model regarding the stability of equilibria, Turing instability, and spatiotemporal Hopf bifurcation induced by two delays.

The remainder of the paper is as follows. In Section 2, we display the model to be discussed in the paper. In Section 3, the existence of the positive equilibrium of system (2.3) and the stability of the unique positive equilibrium are investigated by analyzing the relevant characteristic equations. In Section 4, the existence of Hopf bifurcation is studied by applying the method of stability switching curves given in reference [33]. In Section 5, using the normal form theory and the central manifold theorem, we obtain the direction of Hopf bifurcation and the stability of the bifurcation periodic solutions of the system. In Section 6, the theoretical results are illustrated by performing a series of numerical simulations. Finally, we conclude the paper and give a brief discussion in Section 7.

## 2. Model formulation

In this paper, the base model follows model (2.1) in reference [34], which is a model based on a modified Leslie-Gower predator-prey model with a Beddington-DeAngelis functional response. The detailed and specific reasons that we select the Beddington-DeAngelis functional response is also given in [34]. The Beddington-DeAngelis functional response that embodies predator-prey interactions $\psi(u, v) = \dfrac{qu}{a + bu + cv}$ are as described in [34].

Since the delay can reflect the number fluctuation law of the biological population, the population production has a certain delay, as well as when the population feeds it takes a certain amount of time to digest and absorb. Production delay represents the time lag between predator reproduction and the maturation of offspring; digestion delay corresponds to the time required for predators to process consumed prey into energy available for growth or reproduction [35–37]. For system (1.1), we introduce production delay $\tau_1$ and digestion delay $\tau_2$, and the model is as follows:

$$\begin{cases} \dfrac{\mathrm{d}u}{dt} = ru(1 - \dfrac{u(t-\tau_1)}{K}) - \dfrac{quv}{a + bu + cv}, \\ \dfrac{\mathrm{d}v}{dt} = v(\beta - \dfrac{\gamma v(t-\tau_2)}{u(t-\tau_2) + \alpha}), \end{cases} \tag{2.1}$$

where $a$, $b$, $c$, $q$, $\tau_1$, $\tau_2$ are positive numbers, $q$ is to measure the number of prey that the predator can eat in each time unit, $a$ is the prey density with half-saturated attack rate, $b$ represents the measurement of food abundance relative to the predator population, $c$ is a measure of competition intensity between individuals of the predator population. In the latter part, $u(t-\tau_1)$, $u(t-\tau_2)$, and $v(t-\tau_2)$ can be represented by $u_{\tau_1}$, $u_{\tau_2}$, and $v_{\tau_2}$, respectively.

Based on the analysis in the previous section, the model with cross-diffusion terms can more accurately reflect the predator-prey relationship between predator and prey. Thus we introduce cross-diffusion in model (2.1) and construct the following model under Neumann boundary conditions:

$$\begin{cases} \dfrac{\partial u(x,t)}{\partial t} = d_1\Delta[u(1+\theta v)] + ru(1-\dfrac{u(t-\tau_1)}{K}) - \dfrac{quv}{a+bu+cv}, & 0<x<l\pi,\ t>0,\\ \dfrac{\partial v(x,t)}{\partial t} = d_2\Delta[v(1+\delta u)] + v(\beta - \dfrac{\gamma v(t-\tau_2)}{u(t-\tau_2)+\alpha}), & 0<x<l\pi,\ t>0,\\ u_x(x,t) = v_x(x,t) = 0, & x=0,l\pi,\ t\geq 0,\\ u(x,t) = u_0(x,t) \geq 0, & 0\leq x\leq l\pi,\ -\max\{\tau_1,\tau_2\}\leq t\leq 0,\\ v(x,t) = v_0(x,t) \geq 0, & 0\leq x\leq l\pi,\ -\tau_2\leq t\leq 0, \end{cases} \tag{2.2}$$

where $d_1$ and $d_2$ denote the diffusion coefficients of predator and prey, and they are non-negative numbers. $d_1\theta$ and $d_2\delta$ are cross-diffusion coefficients. $\theta$ and $\delta$ belong to the real number field. The cross-diffusion term can imply different biological significance: $d_1\theta > 0, (d_1\theta < 0)$, depicting a tendency that prey species is far from (resp., close to) high-density areas of predator species; $d_2\delta > 0$ means that the diffusion rate and the population pressure of predator species may weaken in the high density location of prey species. $d_2\delta < 0$, the rate of diffusive spread of predator populations, increases in the process of forming spheres, and the pressure on the predator population enlarges in the center of the sphere. We refer to [32] for more background about the biological explanation regarding the cross-diffusion. The domain inhabited by the species is closed with a one-dimensional length of $l\pi$. Before discussing in detail, we simplify model (2.2) by being dimensionless. The specific scaling process is as follows:

$$\bar{u} = \frac{u}{K},\ \bar{v} = \frac{qv}{bKr},\ \bar{t} = rt,\ d = \frac{a}{Kb},\ d_{11} = \frac{d_1}{r},\ d_{12} = \frac{Krb\theta}{q},$$
$$e = \frac{rc}{q},\ m = \frac{\beta}{r},\ n = \frac{b\gamma}{q},\ p = \frac{\alpha}{K},\ d_{21} = K\delta,\ d_{22} = \frac{d_2}{r}.$$

Dropping the bars, the model (2.2) becomes the following form:

$$\begin{cases} \dfrac{\partial u(x,t)}{\partial t} = d_{11}\Delta[u(1+d_{12}v)] + u(1-u(t-\tau_1)) - \dfrac{uv}{d+u+ev}, & 0<x<l\pi,\ t>0,\\ \dfrac{\partial v(x,t)}{\partial t} = d_{22}\Delta[v(1+d_{21}u)] + v(m - \dfrac{nv(t-\tau_2)}{u(t-\tau_2)+p}), & 0<x<l\pi,\ t>0,\\ u_x(x,t) = v_x(x,t) = 0, & x=0,l\pi,\ t\geq 0,\\ u(x,t) = u_0(x,t) \geq 0, & 0\leq x\leq l\pi,\ -\max\{\tau_1,\tau_2\}\leq t\leq 0,\\ v(x,t) = v_0(x,t) \geq 0, & 0\leq x\leq l\pi,\ -\tau_2\leq t\leq 0, \end{cases} \tag{2.3}$$

where all coefficients are positive numbers expect that $d_{12}$ and $d_{21}$ are real numbers.

In this paper, we work on the effect of feedback delay and digestion delay on the spatio-temporal distribution of model (2.3).

## 3. Existence and stability for the constant steady state

First, we discuss the existence of the coexisting constant steady state of model (2.3). The existence and stability for the constant steady state is a further study of [34]. The existence and the stability of the boundary equilibria are also given in [34]. To avoid excessive length, in the following, we give a summary about the existence and the stability of the boundary equilibria and trivial equilibrium.

**Remark 3.1.** *The constant steady state solution of system* (2.3) *is the same as the equilibria of system* (3.1). *System* (3.1) *always has three boundary equilibria* $(0,0)$, $(1,0)$ *and* $(0, \frac{mp}{n})$.

$$\begin{cases} u(1-u-\dfrac{v}{d+u+ev}) = 0, \\ v(m-\dfrac{nv}{u+p}) = 0. \end{cases} \tag{3.1}$$

- *The origin* $(0,0)$ *is always an unstable node.*
- *The Boundary equilibrium* $(1,0)$ *is always a saddle.*
- *The Boundary equilibrium* $(0, \frac{mp}{n})$ *is always a saddle if* $d > \frac{pm(1-e)}{n}$; $(0, \frac{mp}{n})$ *is always a stable node if* $0 < d < \frac{pm(1-e)}{n}$; $(0, \frac{mp}{n})$ *is always a degenerate equilibrium if* $d = \frac{pm(1-e)}{n}$.

### 3.1. Existence of the positive equilibrium

Let $\bar{E} = (\bar{u}, \bar{v})$ be a positive constant steady-state solution of system (2.3), and the coexisting constant steady state of the system should satisfy the following equation

$$\begin{cases} 1-u-\dfrac{v}{d+u+ev} = 0, \\ m-\dfrac{nv}{u+p} = 0. \end{cases} \tag{3.2}$$

From the second equation of (3.2), we have $\bar{v} = \frac{m(u+p)}{n}$. Bringing it into the first equation, there is

$$m_2u^2 + m_1u + m_0 = 0, \tag{3.3}$$

where

$$m_2 = -(n+em),\ m_1 = n+em-nd-epm-m,\ m_0 = nd+epm-pm.$$

Thus, the system (2.3) has positive equilibria equivalent to Eq (3.3) having positive real roots.

**Theorem 3.2.** *Denote* $\Delta_1 = m_1^2 - 4m_2m_0$. *For the existence of positive roots for* $f(u) = 0$, *we have the following conclusions:*
*(*$H_1$*) If* $\Delta_1 > 0$, $m_0 < 0$, $\frac{m_1}{2m_2} < 0$, *Eq* (3.3) *has two distinct roots* $u_1$, $u_2$.

*($H_2$) If* $\Delta_1 = 0$, $m_0 < 0$, $\dfrac{m_1}{2m_2} < 0$, *Eq* (3.3) *has two identical roots* $u_1 = u_2$.

*($H_3$) As one of the following conditions holds, Eq* (3.3) *always has a positive root* $u_2$.

*(i)* $m_0 > 0$.

*(ii)* $m_0 = 0$, $\dfrac{m_1}{2m_2} < 0$.

*($H_4$) If* $\Delta_1 < 0$, *the Eq* (3.3) *has no positive roots.*

According to Theorem 3.2, there are two constant steady-state solutions when system (2.3) satisfies condition ($H_1$), one constant steady-state solution when system (2.3) satisfies the conditions ($H_2$) and ($H_3$), and no steady-state solution when system (2.3) satisfies the condition ($H_4$).

**Remark 3.3.** *It follows that if either of ($H_2$) and ($H_3$) holds, system* (2.3) *has a unique positive steady-state solution, which is denoted by* $E^* = (u^*, v^*)$.

Regarding the existence, stability, and instability of the positive equilibrium point of the system without diffusion terms and time-delay terms, we present these contents in Section 3 of [34]. We don't elaborate on them here. Next, we will focus on the Turing instability of the positive steady-state solutions.

### *3.2. Stability of the positive steady state*

In the following section, we consider that condition ($H_3$) holds. Linearizing model (2.3) at $E^*$, we have

$$\begin{cases} \dfrac{\partial u(x,t)}{\partial t} = d_{11}\delta_{11}\Delta u + d_{11}\delta_{12}\Delta v + \alpha_{11}u + \alpha_{12}v + \beta_{11}u(x,t-\tau_1), & x \in (0, l\pi), t > 0, \\ \dfrac{\partial v(x,t)}{\partial t} = d_{22}\delta_{21}\Delta u + d_{22}\delta_{22}\Delta v + \beta_{21}u(x,t-\tau_2) + \beta_{22}v(x,t-\tau_2), & x \in (0, l\pi), t > 0, \\ u_x(x,t) = v_x(x,t) = 0, & x = 0, l\pi,\ t \geq 0, \\ u(x,t) = u_0(x,t) \geq 0, & 0 \leq x \leq l\pi,\ -\max\{\tau_1, \tau_2\} \leq t \leq 0, \\ v(x,t) = v_0(x,t) \geq 0, & 0 \leq x \leq l\pi,\ -\tau_2 \leq t \leq 0, \end{cases} \tag{3.4}$$

where

$$\delta_{11} = 1 + d_{12}v^*,\ \delta_{12} = d_{12}u^*,\ \delta_{21} = d_{21}v^*,\ \delta_{22} = 1 + d_{21}u^*,\ \beta_{11} = -u^*,\ \beta_{21} = \frac{nv^{*2}}{(u^* + p)^2},$$

$$\beta_{22} = -\frac{nv^*}{u^* + p},\ \alpha_{11} = 1 - u^* - \frac{v^*(d + ev^*)}{(d + u^* + ev^*)^2},\ \alpha_{12} = -\frac{u^*(d + u^*)}{(d + u^* + ev^*)^2}.$$

Assume that the eigenvector corresponding to the eigenvalues $\lambda$ of (3.4) is

$$(u(t), v(t)) = (c_1, c_2)e^{\lambda t}\cos((\frac{n}{l})x), \tag{3.5}$$

where $n \in N$ is the wavenumber. Substituting (3.4) into Eq (3.5) yields

$$\begin{cases} \lambda c_1 = -d_{11}\delta_{11}c_1(\frac{n}{l})^2 - d_{11}\delta_{12}c_2(\frac{n}{l})^2 + \alpha_{11}c_1 + \alpha_{12}c_2 + \beta_{11}c_1e^{-\lambda\tau_1}, \\ \lambda c_2 = -d_{22}\delta_{21}c_1(\frac{n}{l})^2 - d_{22}\delta_{22}c_2(\frac{n}{l})^2 + \beta_{21}c_1e^{-\lambda\tau_2} + \beta_{22}c_2e^{-\lambda\tau_2}. \end{cases} \tag{3.6}$$

Thus, there are $\lambda(c_1, c_2)^T = J(n; \tau_1, \tau_2)(c_1, c_2)^T$ and

$$J(n; \tau_1, \tau_2) = \begin{pmatrix} -d_{11}\delta_{11}(\frac{n}{l})^2 + \alpha_{11} + \beta_{11}e^{-\lambda\tau_1} & -d_{11}\delta_{12}(\frac{n}{l})^2 + \alpha_{12} \\ -d_{22}\delta_{21}(\frac{n}{l})^2 + \beta_{21}e^{-\lambda\tau_2} & -d_{22}\delta_{22}(\frac{n}{l})^2 + \beta_{22}e^{-\lambda\tau_2} \end{pmatrix},$$

so we can obtain the characteristic equation at the positive equilibrium $(u^*, v^*)$

$$\mathfrak{B}(\lambda; \tau_1, \tau_2) = B_0^n(\lambda) + B_1^n(\lambda)e^{-\lambda\tau_1} + B_2^n(\lambda)e^{-\lambda\tau_2} + B_3^n e^{-\lambda(\tau_1+\tau_2)} = 0, \tag{3.7}$$

where

$$\begin{cases} B_0^n(\lambda) = \lambda^2 + B_{01}^n\lambda + B_{00}^n, \\ B_1^n(\lambda) = B_{11}^n\lambda + B_{10}^n, \\ B_2^n(\lambda) = B_{21}^n\lambda + B_{20}^n, \\ B_3^n = B_{30}^n, \end{cases}$$

for

$$\begin{cases} B_{01}^n = (d_{11}\delta_{11} + d_{22}\delta_{22})(\frac{n}{l})^2 - \alpha_{11}, \\ B_{00}^n = (d_{11}d_{22}\delta_{11}\delta_{22} - d_{11}d_{22}\delta_{12}\delta_{21})(\frac{n}{l})^4 + (d_{22}\delta_{21}\alpha_{12} - d_{22}\delta_{22}\alpha_{11})(\frac{n}{l})^2, \\ B_{11}^n = -\beta_{11}, \\ B_{10}^n = -d_{22}\delta_{22}\beta_{11}(\frac{n}{l})^2, \\ B_{21}^n = -\beta_{22}, \\ B_{20}^n = (\beta_{21}d_{11}\delta_{12} - d_{11}\delta_{11}\beta_{22})(\frac{n}{l})^2 + \beta_{22}\alpha_{11} - \beta_{21}\alpha_{12}, \\ B_{30}^n = \beta_{11}\beta_{22}. \end{cases}$$

3.2.1. Local stability of the positive equilibrium

We investigate the long-time behavior of model (2.3) without time delay and diffusion. In the case of $n = 0$, $\tau_1 = 0$, and $\tau_2 = 0$, Eq (3.7) becomes

$$\lambda^2 - (\alpha_{11} + \beta_{11} + \beta_{22})\lambda + \beta_{22}\alpha_{11} - \beta_{21}\alpha_{12} + \beta_{11}\beta_{22} = 0, \tag{3.8}$$

and the root of (3.8) is given by the following equation

$$\lambda_{1,2} = \frac{(\alpha_{11} + \beta_{11} + \beta_{22}) \pm \sqrt{(\alpha_{11} + \beta_{11} + \beta_{22})^2 - 4(\beta_{22}\alpha_{11} - \beta_{21}\alpha_{12} + \beta_{11}\beta_{22})}}{2}.$$

Due to the complexity of the eigenvalues of the above characteristic equations, it is difficult to directly determine the behavior of the positive equilibrium. Its behavior can be directly determined by the trace and determinant of the Jacobian matrix $J(0; 0, 0)$ at $E^*$.
Let the two eigenvalues of Eq (3.8) be $\lambda_1$ and $\lambda_2$, and there are

$$\lambda_1 + \lambda_2 = \mathrm{tr}(J(0; 0, 0)) = \alpha_{11} + \beta_{11} + \beta_{22},$$

$$\lambda_1\lambda_2 = \det(J(0; 0, 0)) = \beta_{22}\alpha_{11} - \beta_{21}\alpha_{12} + \beta_{11}\beta_{22},$$

so we have the following theorem:

**Theorem 3.4.** *If conditions $H_5$ and $H_6$ hold, where*
$(H_5)$ $\alpha_{11} + \beta_{11} + \beta_{22} < 0$;
$(H_6)$ $\beta_{22}\alpha_{11} - \beta_{21}\alpha_{12} + \beta_{11}\beta_{22} > 0$,
*then Eq* (3.8) *always has two roots of the negative real part. Under the above conditions, the equilibrium $E^*$ of model* (2.3) *is asymptotically stable.*

3.2.2. Turing instability of the positive steady state

Now, we aim to derive the stability for the spatial model (2.3) at $E^*(u^*, v^*)$ without delay. In this case, Eq (3.7) becomes

$$\lambda^2 - \mathrm{tr}(J(n;0,0))\lambda + \det(J(n;0,0)) = 0, \tag{3.9}$$

where

$$\begin{aligned}\mathrm{tr}(J(n;0,0)) &= -(d_{11}\delta_{11} + d_{22}\delta_{22})(\frac{n}{l})^2 + \mathrm{tr}(J(0;0,0)),\\ \det(J(n;0,0)) &= d_{11}d_{22}(\delta_{11}\delta_{22} - \delta_{12}\delta_{21})(\frac{n}{l})^4 + (d_{22}\delta_{21}\alpha_{12} - d_{22}\delta_{22}(\alpha_{11} + \beta_{11})\\ &\quad + \beta_{21}d_{11}\delta_{12} - d_{11}\delta_{11}\beta_{22})(\frac{n}{l})^2 + \det(J(0;0,0)).\end{aligned}$$

Note that $\mathrm{tr}(J(0;0,0)) < 0$ when condition $H_5$ holds. For $\mathrm{tr}(J(n;0,0))$, let

$$(\frac{n}{l})^{2*} = \frac{\mathrm{tr}(J(0;0,0))}{d_{11}\delta_{11} + d_{22}\delta_{22}},\ d_{12}^* = -\frac{1}{v^*} - \frac{d_{22}(1 + d_{21}u^*)}{d_{11}v^*},\ d_{21}^* = -\frac{1}{u^*} - \frac{d_{11}(1 + d_{12}v^*)}{d_{22}u^*},$$

and we have the following cases:

If $d_{12} \geq 0$ and $d_{21} \geq 0$, and one can deduce $d_{11}\delta_{11} + d_{22}\delta_{22} \geq d_{11} + d_{22} > 0$, then $\mathrm{tr}(J(n;0,0)) < 0$.

If $d_{12} < 0$ and $d_{21} < 0$, as $-\frac{1}{v^*} < d_{12} < 0$ and $-\frac{1}{u^*} < d_{21} < 0$, $d_{11}(1 + d_{12}v^*) + d_{22}(1 + d_{21}u^*) > 0$. That is, $d_{11}\delta_{11} + d_{22}\delta_{22} > 0$, and $\mathrm{tr}(J(n;0,0)) < 0$; As $d_{12} < -\frac{1}{v^*}$ and $d_{21} < -\frac{1}{u^*}$, $d_{11}(1 + d_{12}v^*) + d_{22}(1 + d_{21}u^*) < 0$. That is, $d_{11}\delta_{11} + d_{22}\delta_{22} < 0$ can be derived, then $\mathrm{tr}(J(n;0,0)) \geqslant 0$ when condition $(\frac{n}{l})^2 \leq (\frac{n}{l})^{2*}$ is satisfied, and $\mathrm{tr}(J(n;0,0)) < 0$ when condition $(\frac{n}{l})^2 > (\frac{n}{l})^{2*}$ is met.

If $d_{12} < 0$ and $d_{21} > 0$, or $d_{12} > 0$ and $d_{21} < 0$, as $d_{12} < d_{12}^*$ or $d_{21} < d_{21}^*$, $d_{11}(1 + d_{12}v^*) + d_{22}(1 + d_{21}u^*) < 0$, $\mathrm{tr}(J(n;0,0)) \geqslant 0$ when condition $(\frac{n}{l})^2 \leq (\frac{n}{l})^{2*}$ holds, and $\mathrm{tr}(J(n;0,0)) < 0$ when condition $(\frac{n}{l})^2 > (\frac{n}{l})^{2*}$ is met.

Next we consider $\det(J(n;0,0))$ as a quadratic function with respect to $(\frac{n}{l})^2$. Let

$$\mathfrak{D} = d_{11}d_{22}(\delta_{11}\delta_{22} - \delta_{12}\delta_{21}),\ \mathfrak{b} = d_{22}\delta_{21}\alpha_{12} - d_{22}\delta_{22}(\alpha_{11} + \beta_{11}) + \beta_{21}d_{11}\delta_{12} - d_{11}\delta_{11}\beta_{22},$$

As $\mathfrak{D} = 0, \mathfrak{b} < 0$, denote $(\frac{n}{l})_*^2 = \frac{\det(J(0;0,0))}{-\mathfrak{b}}$; As $\mathfrak{D} \neq 0$, denote

$$\Delta_2 = \mathfrak{b}^2 - 4\mathfrak{D}\det(J(0;0,0)),\ (\frac{n}{l})_0^2 = \frac{-\mathfrak{b}}{2\mathfrak{D}},\ (\frac{n}{l})_1^2 = \frac{-\mathfrak{b} - \sqrt{\Delta_2}}{2\mathfrak{D}},\ (\frac{n}{l})_2^2 = \frac{-\mathfrak{b} + \sqrt{\Delta_2}}{2\mathfrak{D}}.$$

We have the following cases:

As $d_{12} > 0$ and $d_{21} > 0$, $d_{11}d_{22}(1+d_{21}u^*+d_{12}v^*) > 0$, and one can derive $\mathfrak{D} > 0$, then $\det(J(n;0,0)) > 0$ if condition $\Delta_2 < 0$ is satisfied; If $\Delta_2 = 0$, $\mathfrak{b} < 0$, then $\det(J(n;0,0)) = 0$ as $(\frac{n}{l})^2 = (\frac{n}{l})_0^2$; If $\Delta_2 > 0$, $\mathfrak{b} < 0$, then $\det(J(n;0,0)) = 0$ as $(\frac{n}{l})^2 = (\frac{n}{l})_1^2$ or $(\frac{n}{l})^2 = (\frac{n}{l})_2^2$, and then $\det(J(n;0,0)) < 0$ as $(\frac{n}{l})_1^2 < (\frac{n}{l})^2 < (\frac{n}{l})_2^2$.

As $d_{12} < 0$ and $d_{21} < 0$, or $d_{12}d_{21} < 0$, if $1 + d_{21}u^* + d_{12}v^* < 0$ and one can deduce $\mathfrak{D} < 0$, $\Delta_2 > 0$, then $\det(J(n;0,0)) > 0$ as $0 < (\frac{n}{l})_2^2 < (\frac{n}{l})_2^2$, $\det(J(n;0,0)) = 0$ as $(\frac{n}{l})_2^2 = (\frac{n}{l})_2^2$, and $\det(J(n;0,0)) < 0$ as $(\frac{n}{l})^2 > (\frac{n}{l})_2^2$.

Summarizing the above discussion, we have the following theorem.

**Theorem 3.5.** *Assuming that conditions* $(H5)$ *and* $(H6)$ *hold, if one of the following conditions is satisfied, then the positive steady-state solution* $E^*$ *changes from asymptotically stable to unstable as the parameter range changes. That is to say, Turing instability of* $E^*$ *emerges.*

$(H_{7a})$ $d_{12} \geq 0$ *and* $d_{21} \geq 0$, $\Delta_2 = 0$, $\mathfrak{b} < 0$, $(\frac{n}{l})^2 = (\frac{n}{l})_0^2$;

$(H_{7b})$ $d_{12} \geq 0$ *and* $d_{21} \geq 0$, $\Delta_2 > 0$, $\mathfrak{b} < 0$, $(\frac{n}{l})_1^2 \leq (\frac{n}{l})^2 \leq (\frac{n}{l})_2^2$;

$(H_{8a})$ $\mathfrak{D} < 0$, $\Delta_2 > 0$, $(\frac{n}{l})^2 \geq (\frac{n}{l})_2^2$;

$(H_{8b})$ $\mathfrak{D} = 0$, $\mathfrak{b} < 0$, $(\frac{n}{l})^2 \geq (\frac{n}{l})_*^2$;

$(H_{9a})$ $d_{11}(1 + d_{12}v^*) + d_{22}(1 + d_{21}u^*) < 0$, $(\frac{n}{l})^2 \leq (\frac{n}{l})^{2*}$, $\mathfrak{D} = 0$, $\mathfrak{b} > 0$;

$(H_{9b})$ $d_{11}(1 + d_{12}v^*) + d_{22}(1 + d_{21}u^*) < 0$, $(\frac{n}{l})^2 \leq (\frac{n}{l})^{2*}$, $\mathfrak{D} > 0$, $\Delta_2 \geq 0$, $\mathfrak{b} < 0$;

$(H_{9c})$ $d_{11}(1 + d_{12}v^*) + d_{22}(1 + d_{21}u^*) < 0$, $(\frac{n}{l})^2 \leq (\frac{n}{l})^{2*}$, $\mathfrak{D} > 0$, $\Delta_2 < 0$;

$(H_{9d})$ $d_{11}(1 + d_{12}v^*) + d_{22}(1 + d_{21}u^*) < 0$, $(\frac{n}{l})^2 \leq (\frac{n}{l})^{2*}$, $\mathfrak{D} < 0$, $\Delta_2 > 0$, $0 \leq (\frac{n}{l})^2 < (\frac{n}{l})_2^2$;

$(H_{9e})$ $d_{11}(1 + d_{12}v^*) + d_{22}(1 + d_{21}u^*) < 0$, $(\frac{n}{l})^2 \leq (\frac{n}{l})^{2*}$, $\mathfrak{D} = 0$, $\mathfrak{b} < 0$, $0 < (\frac{n}{l})^2 \leq (\frac{n}{l})_*^2$.

**Theorem 3.6.** *Assume* $H_5$ *and* $H_6$ *hold. If one of the conditions is satisfied,*

$(H_{10})$ $d_{12} \geq 0$ *and* $d_{21} \geq 0$, $\Delta_2 < 0$;

$(H_{11a})$ $d_{11}(1 + d_{12}v^*) + d_{22}(1 + d_{21}u^*) < 0$, $(\frac{n}{l})^2 > (\frac{n}{l})^{2*}$, $\mathfrak{D} = 0$, $\mathfrak{b} > 0$;

$(H_{11b})$ $d_{11}(1 + d_{12}v^*) + d_{22}(1 + d_{21}u^*) < 0$, $(\frac{n}{l})^2 > (\frac{n}{l})^{2*}$, $\mathfrak{D} > 0$, $\Delta_2 < 0$.

*Then Eq* (3.9) *always has two roots of the negative real part, and the equilibrium* $E^*$ *is asymptotically stable.*

**Remark 3.7.** *If the conditions* $(H_5)$, $(H_6)$, *and* $(H_{7a})$ *or conditions* $(H_5)$, $(H_6)$, *and* $(H_{7b})$ *hold, then* $det(J(n;0,0)) = 0$ *as* $(\frac{n}{l})^2 = (\frac{n}{l})_0^2$, $(\frac{n}{l})^2 = (\frac{n}{l})_1^2$, *or* $(\frac{n}{l})^2 = (\frac{n}{l})_2^2$, *so Eq* (3.9) *possesses a zero eigenvalue, which means that Turing bifurcation occurs [38].*

## 4. Hopf bifurcation

In this section, under the assumption that condition $(H_3)$ holds, we focus on obtaining the existence of Hopf bifurcation for the spatial model (2.3) with two delays $\tau_1$ and $\tau_2$ using the method in [33] to

study the stability switching curves and the crossing directions of the curve.

### *4.1. Stability switching curves*

First, we need to verify whether assumptions $(i)-(iv)$ hold for any fixed $n$ of the characteristic Eq (3.7).

$(i)$ Finite number of characteristic roots on $\mathbb{C}_+ = \{\lambda \in \mathbb{C} : \mathrm{Re}\lambda > 0\}$ under the condition

$$\deg\left(B_0^n(\lambda)\right) \geq \max\left\{\deg\left(B_1^n(\lambda)\right),\ \deg\left(B_2^n(\lambda)\right),\ \deg\left(B_3^n\right)\right\}.$$

$(ii)$ $B_0^n(0) + B_1^n(0) + B_2^n(0) + B_3^n \neq 0$.

$(iii)$ $B_0^n(\lambda)$, $B_1^n(\lambda)$, $B_2^n(\lambda)$ and $B_3^n$ are coprime polynomials.

$(iv)$ $\lim\limits_{\lambda\to\infty}\left(\left|\dfrac{B_1^n(\lambda)}{B_0^n(\lambda)}\right| + \left|\dfrac{B_2^n(\lambda)}{B_0^n(\lambda)}\right| + \left|\dfrac{B_3^n}{B_0^n(\lambda)}\right|\right) < 1.$

The above conditions $(ii)-(iv)$ holds, and $(i)$ follows the [39]. To obtain the stability switching curves, assume that $\lambda = i\omega(\omega > 0)$ is a root of Eq (3.7). Substituting it into the equation, there is

$$\left(B_0^n(i\omega) + B_1^n(i\omega)e^{-i\omega\tau_1}\right) + \left(B_2^n(i\omega) + B_3^n e^{-i\omega\tau_1}\right)e^{-i\omega\tau_2} = 0.$$

Since $\left|e^{-i\omega\tau_2}\right| = 1$, one can get

$$\left|B_0^n(i\omega) + B_1^n(i\omega)e^{-i\omega\tau_1}\right| = \left|B_2^n(i\omega) + B_3^n e^{-i\omega\tau_1}\right|, \tag{4.1}$$

the above equation is equivalent to

$$(B_0^n(i\omega) + B_1^n(i\omega)e^{-i\omega\tau_1})(\bar{B}_0^n(i\omega) + \bar{B}_1^n(i\omega)e^{i\omega\tau_1}) = (B_2^n(i\omega) + B_3^n e^{-i\omega\tau_1})(\bar{B}_2^n(i\omega) + \bar{B}_3^n e^{i\omega\tau_1}).$$

Through simple calculations, we obtain

$$\left|B_0^n(i\omega)\right|^2 + \left|B_1^n(i\omega)\right|^2 - \left|B_2^n(i\omega)\right|^2 - \left|B_3^n\right|^2 = 2A_1^n(\omega)\cos(\omega\tau_1) - 2C_1^n(\omega)\sin(\omega\tau_1), \tag{4.2}$$

where

$$A_1^n(\omega) = \mathrm{Re}(B_2^n(i\omega)\bar{B}_3^n) - \mathrm{Re}(B_0^n(i\omega)\bar{B}_1^n(i\omega)),$$
$$C_1^n(\omega) = \mathrm{Im}(B_2^n(i\omega)\bar{B}_3^n) - \mathrm{Im}(B_0^n(i\omega)\bar{B}_1^n(i\omega)).$$

If there exists $\omega$, such that $A_1^n(\omega)^2 + C_1^n(\omega)^2 = 0$, then we get

$$B_2^n(i\omega)\bar{B}_3^n = B_0^n(i\omega)\bar{B}_1^n(i\omega),\ \ \left|B_0^n(i\omega)\right|^2 + \left|B_1^n(i\omega)\right|^2 = \left|B_2^n(i\omega)\right|^2 + \left|B_3^n\right|^2. \tag{4.3}$$

Therefore, if exists $\omega$ such that (4.3) holds, then all $\tau_1 \in \mathbb{R}_+$ are solutions of Eq (4.1).

If $A_1^n(\omega)^2 + C_1^n(\omega)^2 > 0$, then there is a continuous function $\psi_1^n(\omega)$ such that

$$A_1^n(\omega) = \sqrt{A_1^n(\omega)^2 + C_1^n(\omega)^2}\cos(\psi_1^n(\omega)),$$

$$C_1^n(\omega) = \sqrt{A_1^n(\omega)^2 + C_1^n(\omega)^2}\sin(\psi_1^n(\omega)),$$

where $\psi_1^n(\omega) = \arg\left\{B_2^n(i\omega)\bar{B}_3^n - B_0^n(i\omega)\bar{B}_1^n(i\omega)\right\}$. Thus, Eq (4.2) becomes

$$\left|B_0^n(i\omega)\right|^2 + \left|B_1^n(i\omega)\right|^2 - \left|B_2^n(i\omega)\right|^2 - \left|B_3^n\right|^2 = 2\sqrt{A_1^n(\omega)^2 + C_1^n(\omega)^2}\cos(\psi_1^n(\omega) + \omega\tau_1). \tag{4.4}$$

Thus, there exists $\tau_1 \in \mathbb{R}_+$, satisfying (4.4) equivalent to

$$\left|\left|B_0^n(i\omega)\right|^2 + \left|B_1^n(i\omega)\right|^2 - \left|B_2^n(i\omega)\right|^2 - \left|B_3^n\right|^2\right| \le 2\sqrt{A_1^n(\omega)^2 + C_1^n(\omega)^2}. \tag{4.5}$$

Let the set of $\omega \in \mathbb{R}_+$, satisfying (4.5), be $\Omega_1^n$, and note that (4.5) also includes the case $A_1^n(\omega)^2 + C_1^n(\omega)^2 = 0$. Let

$$\cos(\phi_1^n(\omega)) = \frac{\left|B_0^n(i\omega)\right|^2 + \left|B_1^n(i\omega)\right|^2 - \left|B_2^n(i\omega)\right|^2 - \left|B_3^n\right|^2}{2\sqrt{A_1^n(\omega)^2 + C_1^n(\omega)^2}},\ \phi_1^n(\omega) \in [0, \pi].$$

From the above expression, we have

$$\tau_{1,k_1}^{n\pm}(\omega) = \frac{\pm\phi_1^n(\omega) - \psi_1^n(\omega) + 2k_1\pi}{\omega},\ k_1 \in \mathbb{Z}. \tag{4.6}$$

By the same method as above, one can obtain

$$\tau_{2,k_2}^{n\pm}(\omega) = \frac{\pm\phi_2^n(\omega) - \psi_2^n(\omega) + 2k_2\pi}{\omega},\ k_2 \in \mathbb{Z}, \tag{4.7}$$

where

$$\cos(\phi_2^n(\omega)) = \frac{\left|B_0^n(i\omega)\right|^2 - \left|B_1^n(i\omega)\right|^2 + \left|B_2^n(i\omega)\right|^2 - \left|B_3^n\right|^2}{2\sqrt{A_1^n(\omega)^2 + C_1^n(\omega)^2}},\ \phi_2^n(\omega) \in [0, \pi],$$

$$\psi_2^n(\omega) = \arg\left\{B_1^n(i\omega)\bar{B}_3^n - B_0^n(i\omega)\bar{B}_2^n(i\omega)\right\}.$$

The condition for $\omega$ is as follows

$$\left|\left|B_0^n(i\omega)\right|^2 - \left|B_1^n(i\omega)\right|^2 + \left|B_2^n(i\omega)\right|^2 - \left|B_3^n\right|^2\right| \le 2\sqrt{A_1^n(\omega)^2 + C_1^n(\omega)^2}. \tag{4.8}$$

Let the set of $\omega \in \mathbb{R}_+$, satisfying (4.8), be $\Omega_2^n$. We find that (4.5) is equivalent to (4.8) by squaring both sides of the two conditions (4.5) and (4.8). Therefore, there are $\Omega^n \triangleq \Omega_1^n = \Omega_2^n$, and $\Omega^n$ is called the crossing set of Eq (3.7). Denote

$$\mathcal{F}^n(\omega) \triangleq \left(\left|B_0^n(i\omega)\right|^2 + \left|B_1^n(i\omega)\right|^2 - \left|B_2^n(i\omega)\right|^2 - \left|B_3^n\right|^2\right)^2 - 4\left(A_1^n(\omega)^2 + C_1^n(\omega)^2\right), \tag{4.9}$$

and

$$\Omega^n = \left\{\omega \in \mathbb{R}_+ \middle| \mathcal{F}^n(\omega) \le 0\right\}.$$

**Theorem 4.1.** *The crossing set $\Omega^n$ consists of a finite number of finite-length intervals.*

*Proof.* We demonstrate the above results by a method similar to that in the [33]. From Eq (4.9), it can be seen that $\mathcal{F}^n(\omega)$ is an eighth degree polynomial and $\mathcal{F}^n(+\infty) = +\infty$, so $\mathcal{F}^n(\omega)$ has a finite number of roots on $\mathbb{R}_+$.

If $\mathcal{F}^n(0) > 0$, then the roots of the equation $\mathcal{F}^n(\omega) = 0$ are expressed as $0 < a_1^n < b_1^n \le a_2^n < b_2^n < \cdots \le a_N^n < b_N^n < +\infty$ and

$$\Omega^n = \bigcup_{l=1}^{N} \Omega_{l,n},\ \Omega_{l,n} = [a_l^n, b_l^n].$$

If $\mathcal{F}^n(0) < 0$, then the roots of the equation $\mathcal{F}^n(\omega) = 0$ are expressed as $0 < b_1^n \le a_2^n < b_2^n \le a_3^n < b_3^n < \cdots \le a_N^n < b_N^n < +\infty$ and

$$\Omega^n = \bigcup_{l=1}^{N} \Omega_{l,n},\ \Omega_{1,n} = (0, b_1^n],\ \Omega_{l,n} = [a_l^n,\ b_l^n]\ (l \ge 2).$$

Through the above analysis, the crossing set $\Omega^n$ consists of intervals of finite length.

By verification, we have $\tau_2 = \tau_{2,k_2}^{n-}(\omega)$ when $\tau_1 = \tau_{1,k_1}^{n+}(\omega)$ and $\tau_2 = \tau_{2,k_2}^{n+}(\omega)$ when $\tau_1 = \tau_{1,k_1}^{n-}(\omega)$. Therefore,

$$\mathfrak{T} = \bigcup_{l=1}^{N} \mathfrak{T}_{k_1,k_2}^{n\ \pm l} \cap \mathbb{R}_+^2,\ (k_1 \ge \mathcal{L}_{1,l}, \mathcal{L}_{1,l+1}, \cdots,\ k_2 \ge \mathcal{L}_{2,l}, \mathcal{L}_{2,l+1}, \cdots), \tag{4.10}$$

where $\mathcal{L}_{j,l}$ denotes a lower bound for $k_j$.

$$\begin{aligned} \mathfrak{T}_{k_1,k_2}^{n\ \pm l} &= \left\{ \left( \tau_{1,k_1}^{n\pm}(\omega), \tau_{2,k_2}^{n\mp}(\omega) \right) \middle|\ \omega \in \Omega_{l,n} \right\} \\ &= \left\{ \left( \frac{\pm\phi_1^n(\omega) - \psi_1^n(\omega) + 2k_1\pi}{\omega}, \frac{\mp\phi_2^n(\omega) - \psi_2^n(\omega) + 2k_2\pi}{\omega} \right) \middle|\ \omega \in \Omega_{l,n} \right\}. \end{aligned} \tag{4.11}$$

For any $(\tau_1, \tau_2) \in \mathfrak{T}$ is called a crossing point, and Eq (3.7) has at least one root $i\omega$ with $\omega \in \Omega^n$. The set $\mathfrak{T}$ is the set composed of all the crossing points, which is known as stability switching curves.

Since $\mathcal{F}^n(a_l^n) = \mathcal{F}^n(b_l^n) = 0$, we have

$$\phi_j^n(a_l^n) = \delta_j^a \pi,\ \phi_j^n(b_l^n) = \delta_j^b \pi,$$

where $\delta_j^a, \delta_j^b = 0, 1$ $(j = 1, 2)$. Based on (4.6) and (4.7), we can verify that

$$\left( \tau_{1,k_1}^{n\ +l}(a_l^n), \tau_{2,k_1}^{n\ -l}(a_l^n) \right) = \left( \tau_{1,k_1+\delta_1^a}^{n\ -l}(a_l^n), \tau_{2,k_2-\delta_2^a}^{n\ +l}(a_l^n) \right), \tag{4.12}$$

$$\left( \tau_{1,k_1}^{n\ +l}(b_l^n), \tau_{2,k_1}^{n\ -l}(b_l^n) \right) = \left( \tau_{1,k_1+\delta_1^b}^{n\ -l}(b_l^n), \tau_{2,k_2-\delta_2^b}^{n\ +l}(b_l^n) \right). \tag{4.13}$$

Therefore, for the stability switching curves corresponding to $\Omega_{l,n}$, $\mathfrak{T}_{k_1,k_2}^{n\ +l}$ connects $\mathfrak{T}_{k_1+\delta_1^a,k_2-\delta_2^a}^{n\ -l}$ and $\mathfrak{T}_{k_1+\delta_1^b,k_2-\delta_2^b}^{n\ -l}$ at its ends to $a_l^n$ and $b_l^n$.

Due to Theorem 3.1 in [33], we can directly obtain the following results.

**Theorem 4.2.** *$\mathfrak{T}$ defined in* (4.10) *is the set of all stability switching curves on the $(\tau_1, \tau_2)$ plane of Eq* (3.7)*. In addition, the following conclusions are available:*
*(i) When $\left(\delta_1^a, \delta_2^a\right) = \left(\delta_1^b, \delta_2^b\right)$, $\mathfrak{T}_{k_1,k_2}^{n\ +l}$ and $\mathfrak{T}_{k_1+\delta_1^a,k_2-\delta_2^a}^{n\ -l}$ form a loop on $\mathbb{R}^2$. At this point, $\mathfrak{T}$ is a set of closed continuous curves;*
*(ii) when $\left(\delta_1^a, \delta_2^a\right) \ne \left(\delta_1^b, \delta_2^b\right)$, $\mathfrak{T}$ is a set of continuous curves whose two endpoints either lie on the axes or extend to the infinity region on $\mathbb{R}_+^2$.*

*4.2. Crossing directions*

Assuming that $\lambda = \mu + i\omega$ satisfies Eq (3.7), by the implicit function theorem, $\tau_1$ and $\tau_2$ can be expressed as functions of $\mu$ and $\omega$. As $\lambda = i\omega$, denote $\mathfrak{B}(\lambda;\tau_1,\tau_2)$ as $\mathfrak{B}(i\omega)$. Thus, we have the following expressions:

$$\begin{aligned}
\frac{\partial \mathrm{Re}\ \mathfrak{B}(i\omega)}{\partial \mu} =& \mathrm{Re}\left\{B_0^{n'}(i\omega) + \sum_{k=1}^{2}\left(B_k^{n'}(i\omega) - \tau_k B_k^n(i\omega)\right)e^{-i\omega\tau_k} - (\tau_1+\tau_2)B_3^n e^{-i\omega(\tau_1+\tau_2)}\right\} = \mathcal{R}_0,\\
\frac{\partial \mathrm{Im}\ \mathfrak{B}(i\omega)}{\partial \mu} =& \mathrm{Im}\left\{B_0^{n'}(i\omega) + \sum_{k=1}^{2}\left(B_k^{n'}(i\omega) - \tau_k B_k^n(i\omega)\right)e^{-i\omega\tau_k} - (\tau_1+\tau_2)B_3^n e^{-i\omega(\tau_1+\tau_2)}\right\} = \mathcal{I}_0,\\
\frac{\partial \mathrm{Re}\ \mathfrak{B}(i\omega)}{\partial \tau_1} =& \mathrm{Re}\left\{-i\omega\left(B_1^n(i\omega)e^{-i\omega\tau_1} + B_3^n e^{-i\omega(\tau_1+\tau_2)}\right)\right\} = \mathcal{R}_1,\\
\frac{\partial \mathrm{Im}\ \mathfrak{B}(i\omega)}{\partial \tau_1} =& \mathrm{Im}\left\{-i\omega\left(B_1^n(i\omega)e^{-i\omega\tau_1} + B_3^n e^{-i\omega(\tau_1+\tau_2)}\right)\right\} = \mathcal{I}_1,\\
\frac{\partial \mathrm{Re}\ \mathfrak{B}(i\omega)}{\partial \tau_2} =& \mathrm{Re}\left\{-i\omega\left(B_2^n(i\omega)e^{-i\omega\tau_2} + B_3^n e^{-i\omega(\tau_1+\tau_2)}\right)\right\} = \mathcal{R}_2,\\
\frac{\partial \mathrm{Im}\ \mathfrak{B}(i\omega)}{\partial \tau_2} =& \mathrm{Im}\left\{-i\omega\left(B_2^n(i\omega)e^{-i\omega\tau_2} + B_3^n e^{-i\omega(\tau_1+\tau_2)}\right)\right\} = \mathcal{I}_2,\\
\frac{\partial \mathrm{Re}\ \mathfrak{B}(i\omega)}{\partial \omega} =& -\mathcal{I}_0,\ \frac{\partial \mathrm{Im}\ \mathfrak{B}(i\omega)}{\partial \omega} = \mathcal{R}_0.
\end{aligned}$$

If $\det\begin{pmatrix}\mathcal{R}_1 & \mathcal{R}_2\\ \mathcal{I}_1 & \mathcal{I}_2\end{pmatrix} = \mathcal{R}_1\mathcal{I}_2 - \mathcal{R}_2\mathcal{I}_1 \neq 0$, through the implicit function theorem, then

$$\Delta(\omega) \triangleq \left.\begin{pmatrix}\frac{\partial\tau_1}{\partial\mu} & \frac{\partial\tau_1}{\partial\omega}\\ \frac{\partial\tau_2}{\partial\mu} & \frac{\partial\tau_2}{\partial\omega}\end{pmatrix}\right|_{\mu=0,\omega\in\Omega^n} = -\begin{pmatrix}\mathcal{R}_1 & \mathcal{R}_2\\ \mathcal{I}_1 & \mathcal{I}_2\end{pmatrix}^{-1}\begin{pmatrix}\mathcal{R}_0 & -\mathcal{I}_0\\ \mathcal{I}_0 & \mathcal{R}_0\end{pmatrix}. \tag{4.14}$$

For an arbitrary stability switching curve $\mathfrak{T}^{n\ \pm l}_{k_1,k_2}$, the direction of the curve corresponding to the increase in $\omega \in \Omega_{l,n}$ is called the positive direction. We call the region on the left-hand (right-hand) side the left (right) region when the curve moves in a positive direction. Since the tangent vector of $\mathfrak{T}^{n\ \pm l}_{k_1,k_2}$ along the positive direction of the curve is $\left(\frac{\partial\tau_1}{\partial\omega}, \frac{\partial\tau_2}{\partial\omega}\right)$, the normal vector of $\mathfrak{T}^{n\ \pm l}_{k_1,k_2}$ pointing to the right region is $\left(\frac{\partial\tau_2}{\partial\omega}, -\frac{\partial\tau_1}{\partial\omega}\right)$. When a pair of complex eigenvalues cross the imaginary axis on the complex plane to the right with the change of $\mu$, it is obvious that $(\tau_1,\tau_2)$ moves along the direction of $\left(\frac{\partial\tau_1}{\partial\mu}, \frac{\partial\tau_2}{\partial\mu}\right)$. If the inner product of the following two vectors is positive,

$$\delta(\omega) \triangleq \left(\frac{\partial\tau_1}{\partial\mu}, \frac{\partial\tau_2}{\partial\mu}\right)\left(\frac{\partial\tau_2}{\partial\omega}, -\frac{\partial\tau_1}{\partial\omega}\right) = \frac{\partial\tau_1}{\partial\mu}\frac{\partial\tau_2}{\partial\omega} - \frac{\partial\tau_2}{\partial\mu}\frac{\partial\tau_1}{\partial\omega} > 0, \tag{4.15}$$

then Eq (3.7) has two more characteristic roots with positive real parts in the region to the right of $\mathfrak{T}^{n\ \pm l}_{k_1,k_2}$. If inequality (4.15) is reversed, then Eq (3.7) has two more characteristic roots with positive real parts in the region to the left of $\mathfrak{T}^{n\ \pm l}_{k_1,k_2}$.

It is obvious to see that $\delta(\omega) = \det\Delta(\omega)$, and $\det\begin{pmatrix}-\mathcal{R}_0 & \mathcal{I}_0\\ -\mathcal{I}_0 & -\mathcal{R}_0\end{pmatrix} = \mathcal{R}_0^2 + \mathcal{I}_0^2 \geq 0$, so the sign of $\delta(\omega)$ is determined by the range of $\mathcal{R}_1\mathcal{I}_2 - \mathcal{R}_2\mathcal{I}_1$. If either $\mathcal{R}_0 \neq 0$ or $\mathcal{I}_0 \neq 0$, it holds without considering that

$i\omega$ is the multiple root of Eq (3.7). By further calculation, we obtain

$$\begin{aligned}
&\mathcal{R}_1\mathcal{I}_2 - \mathcal{R}_2\mathcal{I}_1 \\
&= \mathrm{Im}\left\{\overline{-i\omega\left(B_1^n e^{-i\omega\tau_{1,k_1}^{n\pm}} + B_3^n e^{-i\omega(\tau_{1,k_1}^{n\pm}+\tau_{2,k_2}^{n\mp})}\right)}(-i\omega)\times\left(B_2^n e^{-i\omega\tau_{2,k_2}^{n\mp}} + B_3^n e^{-i\omega(\tau_{1,k_1}^{n\pm}+\tau_{2,k_2}^{n\mp})}\right)\right\} \\
&= \omega^2\mathrm{Im}\left\{\left(B_2^n\overline{B_3^n} - B_0^n\overline{B_1^n}\right)e^{i\omega\tau_{1,k_1}^{n\pm}}\right\} \\
&= \pm\omega^2\left|B_2^n\overline{B_3^n} - B_0^n\overline{B_1^n}\right|\sin\phi_1^n.
\end{aligned}$$

Therefore,

$$\mathrm{sign}\ \delta(\omega\in\mathring{\Omega}_{l,n}) = \pm\mathrm{sign}\left\{\omega^2\left|B_2^n\overline{B_3^n} - B_0^n\overline{B_1^n}\right|\sin\phi_1^n\right\} = \pm 1, \tag{4.16}$$

where $\phi_1^n(\mathring{\Omega}_{l,n}) \subset (0,\pi)$, and $\mathring{\Omega}_{l,n}$ indicates the interior of $\Omega_{l,n}$. Equation (4.16) indicates that they have different stability switching directions, which means that when we move along these continuous curves, the stability switching directions are consistent.

From the above analysis and by combining Theorem 4.1 of the [33], we can directly obtain the following results.

**Lemma 4.3.** *For arbitrary l=1, 2$\cdots$N, we have*

$$sign\ \delta(\omega\in\mathring{\Omega}_{l,n}) \triangleq \pm 1,\ \forall\,(\tau_1(\omega),\tau_2(\omega)) \in \mathfrak{T}_{k_1,k_2}^{n\ \pm l}.$$

*Therefore, the region to the left of $\mathfrak{T}_{k_1,k_2}^{n\ +l}$ ($\mathfrak{T}_{k_1,k_2}^{n\ -l}$) has two more (fewer) characteristic roots with positive real parts.*

Based on the above discussion, we have introduced the following conclusion about the existence of the Hopf bifurcation [40].

**Theorem 4.4.** *$\mathfrak{T}$ is a Hopf bifurcation curve in the following cases: For any $\varsigma\in\mathfrak{T}$ and for any smooth curve $F$ intersecting with $\varsigma\in\mathfrak{T}$ transversely at $\varsigma$, we define the tangent of $F$ at $\varsigma$ by $\vec{z}$. If $\frac{\partial Re\lambda}{\partial\vec{z}}\Big|_{\varsigma}\neq 0$, and the other eigenvalues of* (3.7) *at $\varsigma$ have nonzero real parts, then system* (2.3) *undergoes a Hopf bifurcation at $\varsigma$ when parameters $(\tau_1,\tau_2)$ cross $\mathfrak{T}$ at $\varsigma$ along $F$.*

## 5. The direction and stability of bifurcation periodic solutions

In Section 4, we know that the positive equilibrium $E^*$ of the system (2.3) undergoes a Hopf bifurcation at any critical values $(\tau_1,\tau_2) = (\tau_1^*,\tau_2^*) \in \mathfrak{T}$ for $n = n_s$. This section extends the method proposed in [35, 41, 42] to system (2.3), calculate the normal form of the model at the positive equilibrium $E^*$ to further determine the direction of Hopf bifurcation and the stability of the bifurcation periodic solutions. Without loss of generality, we always assume that $\tau_1 > \tau_2$, and the case $\tau_1 < \tau_2$ can be carried out in a similar form. We fix $\tau_2 = \tau_2^*$, and denote the value of $\omega$ to $(\tau_1^*,\tau_2^*)$ as $\omega^*$. For convenience of representation, the latter part $\tau_2^*$, $\tau_1^*$ and $\omega^*$ is represented by $\tau_2$, $\tau^*$, and $\omega$. Before making the calculations of the normal form, we need to introduce some basic notation and equation transformation.

### 5.1. The basic notations and equation transformation

In this subsection, we introduce some convention symbols used in [35, 41, 42] and define the following real-valued Hilbert space

$$X = \{U = (u_1, u_2) \in H^2(0, l\pi) \oplus H^2(0, l\pi) : \frac{\partial u_1}{\partial x} = \frac{\partial u_2}{\partial x} = 0, x = 0, l\pi\},$$

and its inner product is defined as

$$[U, V] = \int_0^{l\pi} U^T V \mathrm{d}x, \text{ for } U, V \in X.$$

Let $M = C([-\max\{1, \frac{\tau_2}{\tau_1}\}, 0]; X)$, and it is a Banach space with a continuous mapping from $[-\max\{1, \frac{\tau_2}{\tau_1}\}, 0]$ to $X$.
Denote

$$b_n(x) = \frac{\cos(\frac{n}{l}x)}{\left\|\cos(\frac{n}{l}x)\right\|_{L^2}} = \begin{cases} \sqrt{\frac{1}{l\pi}}, & n = 0, \\ \sqrt{\frac{2}{l\pi}}\cos(\frac{n}{l}x), & n \geq 1. \end{cases}$$

Set $\beta_n^{(1)} = (b_n, 0)^T, \beta_n^{(2)} = (0, b_n)^T$.
By setting $\tau_1 = \tau^* + \zeta$, $\zeta \ll 1$ is a small perturbation of $\tau^*$ is such that $\zeta = 0$ is the Hopf bifurcation value of model (2.3). In addition, in the following calculations, $\zeta$ is considered a state variable.

Make the following transformation to shift $E^*(u^*, v^*)$ to the origin

$$\begin{cases} u_1(x, t) = u(x, t) - u^*, \\ u_2(x, t) = v(x, t) - v^*, \end{cases}$$

and normalize the delay by rescaling the time variable $t \to \frac{t}{\tau_1}$. Let $U(x, t) = (u_1(x, t), u_2(x, t))^T$. We rewrite $U(x, t)$ as $U(t)$ and $U_t(\kappa) = U_t(x, t + \kappa)$ as $U_t$, where $-\max\{1, \frac{\tau_2}{\tau_1}\} \leq \kappa \leq 0$ and $U_t \in X$.

### 5.2. The normal form

Based on the calculation in Appendix A and Appendix B, we obtain the normal form of Hopf bifurcation as shown below

$$\dot{m} = \mathcal{V}m + \frac{1}{2}\begin{pmatrix} N_1 m_1 \zeta \\ \bar{N}_1 m_2 \zeta \end{pmatrix} + \frac{1}{3!}\begin{pmatrix} N_2 m_1^2 m_2 \\ \bar{N}_2 m_1 m_2^2 \end{pmatrix} + O\left(|m|\,\zeta^2 + |m|^4\right), \tag{5.1}$$

where

$$N_1 = 2p^T(0)\left(A_1 q(0) + A_2 q(-1) + (1 + i\omega\tau_2)A_3 q(-\frac{\tau_2}{\tau^*}) - \left(\frac{n_s}{l}\right)^2 B_1 q(0)\right),$$

$$N_2 = N_{21} + \frac{3}{2}(N_{22} + N_{23} + N_{24}).$$

According to references [41] and [42], we can rewrite Eq (5.1) as

$$\dot{\sigma} = \mathcal{K}_1 \sigma\zeta + \mathcal{K}_2 \sigma^3 + O\left(\zeta^2\sigma + |(\sigma, \zeta)|^4\right),$$

where

$$\mathcal{K}_1 = \frac{1}{2}Re(N_1), \quad \mathcal{K}_2 = \frac{1}{3!}Re(N_2).$$

According to [43], we know that the symbols of $\mathcal{K}_1$ and $\mathcal{K}_2$ can determine the direction of Hopf bifurcation and the stability of periodic solutions. Therefore, based on the previous analysis, we infer the following theorem:

**Theorem 5.1.** *The sign of $\mathcal{K}_1\mathcal{K}_2$ determines the direction of Hopf bifurcation, while the sign of $\mathcal{K}_2$ determines the stability of the periodic solution of Hopf bifurcation. The main situation is as follows: 1) Hopf bifurcation is supercritical when $\mathcal{K}_1\mathcal{K}_2 < 0$, Hopf bifurcation is subcritical when $\mathcal{K}_1\mathcal{K}_2 > 0$. 2) The periodic solution of Hopf bifurcation is stable when $\mathcal{K}_2 < 0$, the periodic solution of Hopf bifurcation is unstable when $\mathcal{K}_2 > 0$.*

The calculation process of the coefficients corresponding to the above theorem is shown in the Appendix.

## 6. Numerical simulations

In this section, we give some numerical simulations to verify the findings of this paper. The numerical simulations about the existence, stability, and instability for the positive equilibrium point and boundary equilibria of the system without diffusion and delay are shown in [34]. Here, we omit it.

In the numerical simulations, we choose the parameters in the model (2.2) as $n = 0.8$, $d = 1.2$, $e = 0.5$, $p = 0.6$, $m = 0.4$, $d_{11} = 0.13$, and $d_{22} = 0.13$. By changing the value of $d_{12}$ and $d_{21}$, we can obtain Turing instability of $E^* = (0.7074, 0.6537)$.

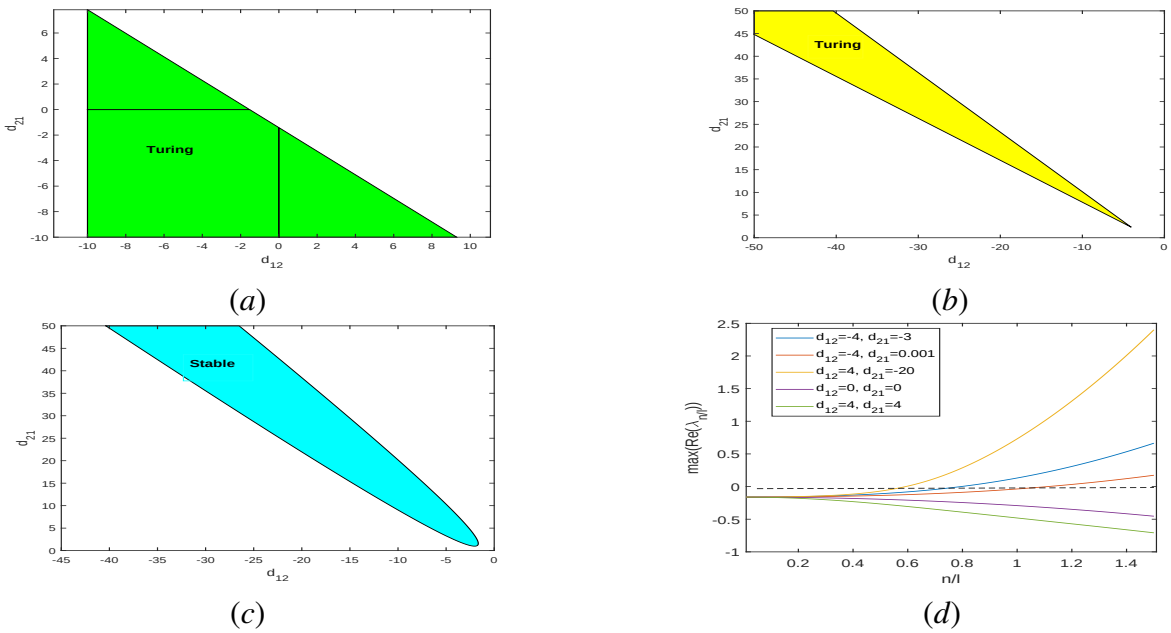


(*a*) (*b*) (*c*) (*d*)

**Figure 1.** Turing instability of $E^*$.

By Theorem 3.5, as $(d_{12}, d_{21})$ takes the value from $(-10, -10)$ to $(10, 10)$, condition $(H_{8a})$ holds, and the Turing region is displayed as the green field in Figure 1(*a*). As $(d_{12}, d_{21})$ takes the value from

$(-50,-50)$ to $(50,50)$, condition $(H_{9b})$ holds, and the Turing region is displayed as the yellow field in $(b)$ in Figure 1. By Theorem 3.6, as $(d_{12},d_{21})$ takes the value from $(-50,-50)$ to $(50,50)$, condition $(H_{11b})$ holds, and the stable region is displayed as the cyan field in Figure 1$(c)$. Take $(d_{12},d_{21})$ as $(4,4)$, $(0,0)$, $(4,-20)$, $(-4,0.001)$, and $(-4,-3)$. As $(d_{12},d_{21})=(4,4)$, condition $(H_{10})$ holds, and $E^*$ is asymptotically stable; as $(d_{12},d_{21})=(0,0)$, conditions $(H_5)$ and $(H_6)$ holds, and $E^*$ is asymptotically stable; As $(d_{12},d_{21})=(4,-20)$, condition $(H_{8a})$ holds, and Turing instability appear; as $(d_{12},d_{21})=(-4,0.001)$, condition $(H_{9b})$ holds, and Turing instability appears; as $(d_{12},d_{21})=(-4,-3)$, condition $(H_{8a})$ holds, and Turing instability appears. In Figure 1$(d)$, one can directly see that the real part of the maximum eigenvalue of (3.9) is always negative as $(4,4)$ and $(0,0)$, so the equilibrium $E^*$ is asymptotically stable. However, when $(d_{12},d_{21})$ takes $(4,-20)$, $(-4,0.001)$ and $(-4,-3)$, the real part of the maximum eigenvalue of (3.9) changes positive from negative, that is, Turing instability appears.

As $n=0.8$, $d=1.2$, $e=0.5$, $p=0.6$, $m=0.4$, $d_{11}=0.13$, $d_{22}=0.13$, $n=1$, $\tau_1=13$, $\tau_2=6$, as $d_{12}=4$, and $d_{21}=4$, one can see $E^*=(0.7074,0.6537)$ is stable (see Figure 2$(a)$,$(b)$) and as $d_{12}=-4$, $d_{21}=-3$, one can obtain that $E^*$ is unstable (see Figure 2$(c)$,$(d)$). For Panel (a): The surface fluctuates slightly around $(u^*=0.7074)$ (the $z-$axis range is $0.7-0.8$) and maintains spatial homogeneity (no distinct patterns form across the $x-$axis). For Panel (b): $v(x,t)$ oscillates near $v^*=0.6537$ (the $z-$axis range is $0.66-0.74$ with no spatial heterogeneity. These results confirm that $E^*$ is asymptotically stable under this parameter set: Small initial perturbations decay, and the system remains near the equilibrium. For Panel (c): The surface deviates sharply from $u^*$: Initial small fluctuations (near $t=0$) grow into spatially heterogeneous patterns (striped structures along the $x-$axis). The $z-$axis range expands to $0-5$, indicating large deviations from $E^*$. For Panel (d): $v(x,t)$ exhibits analogous behavior-small initial perturbations evolve into distinct spatial patterns, with the $z-$axis range also expanding to $0-5$. This transition from homogeneous, small fluctuations (Panels (a) and (b)) to heterogeneous, large-amplitude patterns (Panels (c) and (d)) directly demonstrates that $E^*$ becomes Turing-unstable under $d_{12}=-4,d_{21}=-3$.

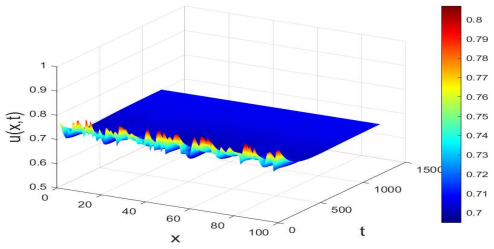


$(a)$ $d_{12}=4$, $d_{21}=4$

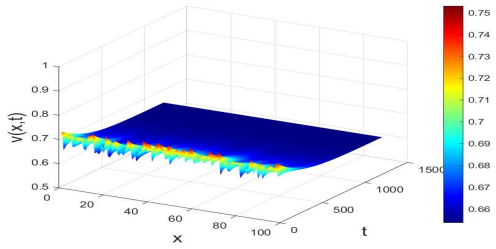


$(b)$ $d_{12}=4$, $d_{21}=4$

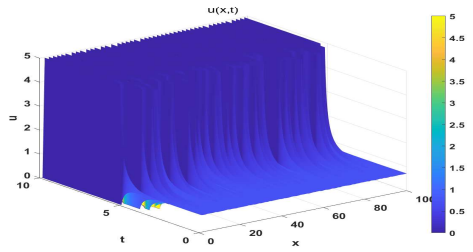


$(c)$ $d_{12}=-4$, $d_{21}=-3$

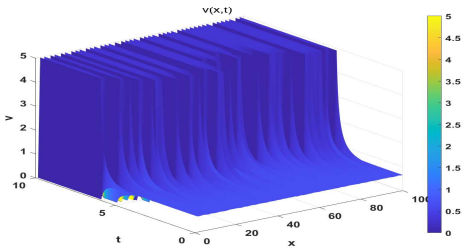


$(d)$ $d_{12}=-4$, $d_{21}=-3$

**Figure 2.** Turing instability of $E^*$.

Next, we focus on the pattern formation of $E^*$. As $d_{12} = -4$, $d_{21} = -3$, the parameter group satisfies conditions $(H_5)$, $(H_6)$, and $(H_{8a})$, and a Turing pattern of $E^* = (0.7074, 0.6537)$ appears. The situations of other diffusion parameters can be obtained in a similar way. Thus, we choose the initial value as $u_0 = 0.7074 + 0.02 * rand(1, M)$ and $v_0 = 0.6537 + 0.02 * rand(1, M)$ with $M = 100$.

Start pattern formation with a homogeneous steady state solution at $nt = 1$, which almost equals to the case that $d_{11} = d_{12} = d_{21} = d_{22} = 0$. One can conclude that $E^*$ is stable and obtains the stationary pattern shown in $(a)$ in Figures 3 and 4. As time $T$ increases, $d_{11}d_{12}d_{21}d_{22} \neq 0$, Turing instability and heterogeneous pattern formation of system (2.2) around $E^*$ appear (see $(b) - (f)$ of Figures 3 and 4).

At $nt = 1$, $(u(x,t), v(x,t))$ starts near the stable equilibrium $E^*$, exhibiting only small, uniform spatial fluctuations-this reflects the initial stable regime (small perturbations decay, and the system remains homogeneous). By $nt = 100$, subtle spatial variations emerge (faint striped structures along $x$), signaling the onset of Turing instability: Cross-diffusion begins to amplify small inhomogeneities, pushing the system away from the uniform steady state. As $nt$ increases to $200 - 250$, these variations grow into distinct, organized spatial patterns (pronounced stripes), confirming the loss of stability. By $nt = 400$, $(u(x,t), v(x,t))$ forms robust, large-amplitude heterogeneous structures (dense patches and sparse regions), with values deviating significantly from $E^*$. This final state embodies the Turing-unstable regime, where cross-diffusion sustains persistent spatial heterogeneity (no return to uniformity). In short, Figures 3 and 4 trace the classic Turing instability cascade: From stable homogeneity to incipient spatial variation, and finally to fully developed heterogeneous patterns, which is driven by cross-diffusion-induced breakdown of the uniform equilibrium.

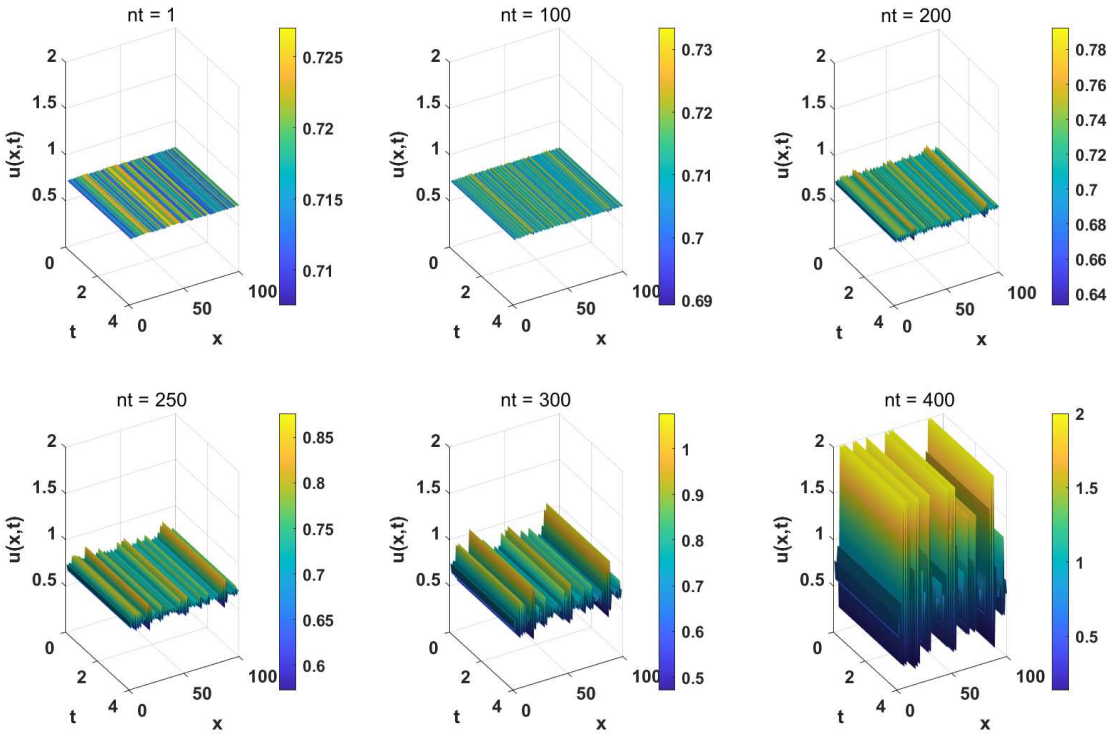


**Figure 3.** The pattern formation of $u$ as $d_{11} = 0.13$, $d_{12} = -4$, $d_{21} = -3$, $d_{22} = 0.13$.

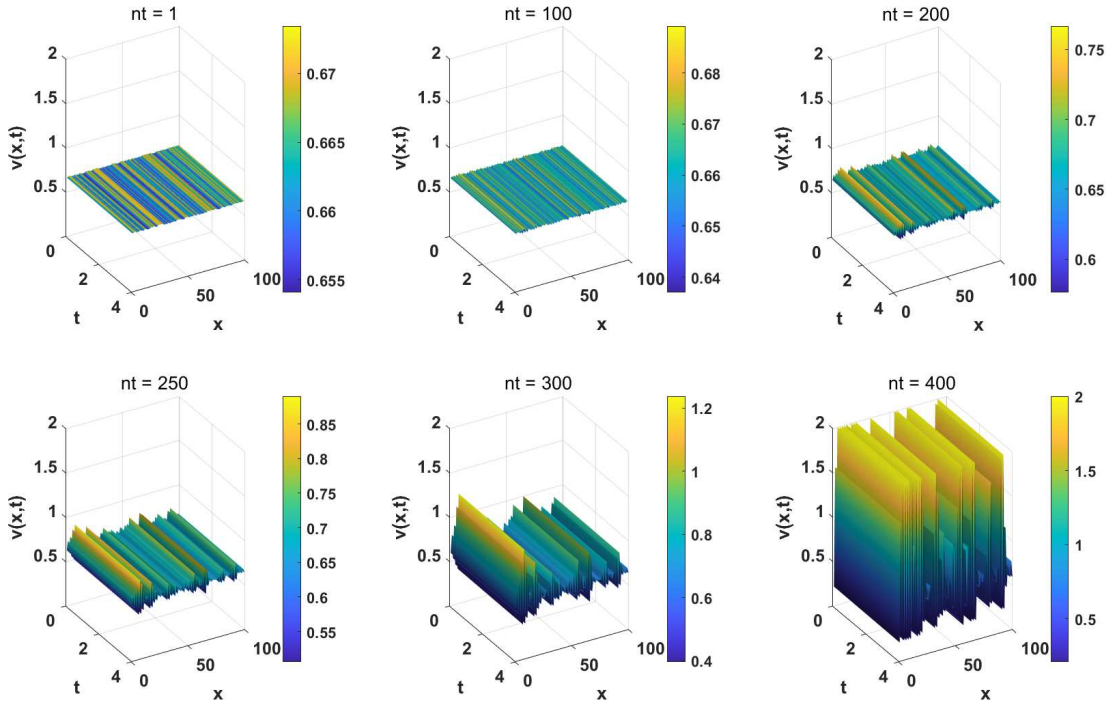


**Figure 4.** The pattern formation of $v$ as $d_{11} = 0.13$, $d_{12} = -4$, $d_{21} = -3$, $d_{22} = 0.13$.

Next, the parameters are chosen as

$$n = 0.6,\ d = 0.9,\ e = 0.8,\ p = 0.6,\ m = 0.4,$$
$$l = 2,\ d_{11} = 0.6,\ d_{12} = 0.3,\ d_{21} = 0.4,\ d_{22} = 5,$$

and we can obtain the unique positive constant equilibrium $E^* = (0.5291, 0.7527)$, and the equilibrium $E^*$ is always stable. To illustrate the dynamics in the presence of delays, we apply the procedure given in Section 4 for verification. $\mathcal{F}^1(\omega)$ has only two roots $a_1^1 \approx 0.4831$, $a_2^1 \approx 0.5654$, as shown in $(a)$ of Figure 5, and

$$\delta_1^a = 0,\ \delta_2^a = 1,\ \delta_1^b = 1,\ \delta_2^b = 1.$$

From Theorem 4.2, we can determine that the switching curves belong to class (ii). As $\tau_1$ and $\tau_2$ vary, we can determine the cross direction of the characteristic roots according to Lemma 4.3, as shown in $(b)$ of Figure 5. We can investigate the direction and stability of the Hopf bifurcation based on the procedure in Section 5. When $n = 1$, by further calculations $\tau_1 = \tau_1^* = 14.4975$ and $\tau_2 = \tau_2^* = 5.3208$, for the above critical Hopf bifurcation values, we have

$$\mathcal{K}_1 = 0.0810 > 0,\ \mathcal{K}_2 = -0.0243 < 0,$$

which implies that the mode-1 spatial inhomogeneous Hopf bifurcation at $\tau_1^*$ and $\tau_2^*$ are supercritical and stable. When $\tau_1 = \tau_1^*$, $\tau_2 = \tau_2^*$, the inhomogeneous Hopf bifurcation is stable, whose figure is displayed in Figure 6$(a)$,$(b)$. When $\tau_1 = 15 > \tau_1^*$, $\tau_2 = 6 > \tau_2^*$, the inhomogeneous Hopf bifurcation is unstable and converges to $E^*$, whose figure is displayed in Figure 6$(c)$,$(d)$.

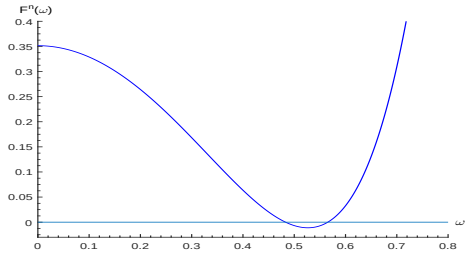


($a$) Graph of $\mathcal{F}^n(\omega)$

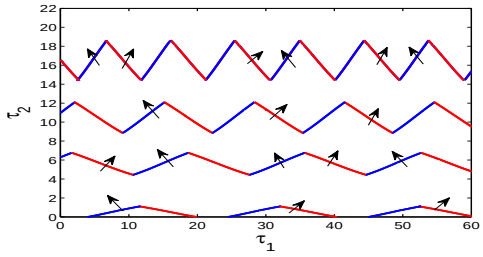


($b$) Stability switching curves $\mathfrak{T}$.

**Figure 5.** Stability switching curves.

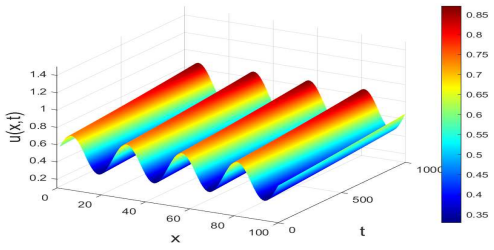


($a$) $\tau_1 = 14.4975,\ \tau_2 = 5.3208,\ nt = 1000$

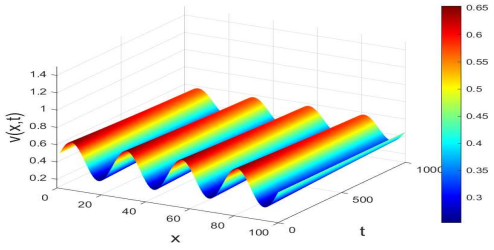


($b$) $\tau_1 = 14.4975,\ \tau_2 = 5.3208,\ nt = 1000.$

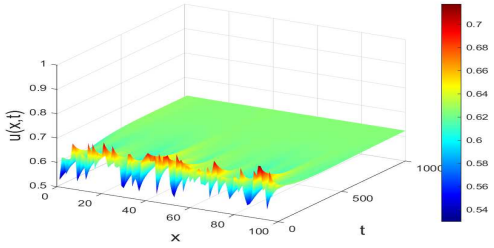


($c$) $\tau_1 = 15,\ \tau_2 = 6,\ nt = 1000$

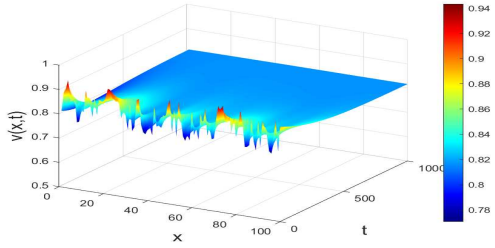


($d$) $\tau_1 = 15,\ \tau_2 = 6,\ nt = 1000.$

**Figure 6.** Bifurcation near $E^*$.

## 7. Conclusions

In this paper, we deal with a predator-prey model with two delays and cross-diffusion. Through theoretical analysis, we obtain some sufficient conditions for the Turing instability at positive equilibrium. Numerical calculations verify the case of Turing instability. Over time, the stability of the steady state solution of the system changes from stable to unstable, and the time increases up to a certain point where the solution curve diverges and tends to infinity.

Drawing on the stability crossing curves method proposed in [33], we obtain stability crossing curves in the $(\tau_1, \tau_2)$ plane. When $(\tau_1, \tau_2)$ lies on the crossing curves, the characteristic Eq (3.7) has at least one pair of pure imaginary roots, so we identify the stable region of positive equilibrium. Furthermore, taking $\tau_1, \tau_2$ as the bifurcation parameter, the conditions for the existence of Hopf bifurcation are obtained. Based on the emergence of Hopf bifurcation and combined with the central manifold theorem and the normal form theory, by calculating the coefficients of the normal form, the determining conditions for the Hopf bifurcation direction and the stability of the bifurcation periodic

solutions are further determined, and the corresponding theorems are given.

Turing patterns describe the formation mechanism of spatial heterogeneity in ecology. By introducing cross-diffusion terms, the paper reveals how populations in a uniform habitat can spontaneously form non-uniform spatial distribution patterns (e.g., patches, stripes) through the coupling of diffusion and local interactions (such as predation and competition). The specific ecological implications include: When the system satisfies the Turing instability conditions (e.g., conditions $(H_{7a}) - (H_{9e})$ in Theorem 3.5 of the paper), the homogeneous steady-state solution $E$ becomes unstable, and the spatial distribution transitions from a uniform state to an ordered patchy distribution (as shown in the numerical simulations in Figures 1–4 of the paper). For instance, the spatial separation of predators and prey may reduce competitive pressure and promote the maintenance of biodiversity. Numerical simulations in Section 6 demonstrate that when diffusion parameters meet specific conditions (e.g., $d_{12} = -4$ and $d_{21} = -3$), the system exhibits Turing patterns (Figures 3 and 4), simulating the aggregated distribution of species in natural ecosystems.

We focus on the coupling effects of two types of delays: The production delay (reflecting the population's reproduction maturation time) and the digestion delay (reflecting the predator's digestion and absorption process). Their interaction leads to periodic oscillations in the system through Hopf bifurcation (Sections 4 and 5), with specific mechanisms as follows: The coupling of delays introduces phase differences, amplifying system fluctuations. For example, in the characteristic Eq (3.7), the superposition of delay terms $e^{-\lambda\tau_1}$ and $e^{-\lambda\tau_2}$ may transition the system from a stable equilibrium (Theorem 3.4) to a Hopf bifurcation (Theorem 4.4), generating periodic oscillations. Numerical simulations (Figures 5 and 6) show that when the delay combination $(\tau_1, \tau_2)$ crosses the stability switching curves, the system transitions from a stable state (Figures 6(a),(b)) to periodic oscillations (Figures 6(c),(d)), demonstrating the regulatory role of delay coupling on population dynamics. Stable periodic solutions (e.g., limit cycles) represent predictable periodic fluctuations in population numbers (such as seasonal fluctuations), indicating ecosystem resilience. In Section 5, the stability of periodic solutions is determined by calculating the normal form coefficient $K_2$ (Theorem 5.1; the solution is stable when $K_2 < 0$). Unstable periodic solutions: Indicate critical thresholds where minor disturbances may lead to population collapse or outbreaks. For example, when delay parameters approach the bifurcation curve (Figure 5), the system becomes highly sensitive to environmental fluctuations, explaining phenomena such as sudden species extinction or invasion.

Moreover, several other promising avenues for future investigation remain open. For instance:
(i) Introducing stochastic perturbations: Incorporating environmental noise or random fluctuations into the model could enable us to analyze the robustness and dynamic behavior of the system under stochastic influences, which is often more realistic for ecological settings.
(ii) Extending to heterogeneous spatial environments: Studying the effects of cross-diffusion and delays in non-uniform media, such as landscapes with spatially varying resource distributions or habitat fragmentation, could provide insights into pattern formation in real-world ecosystems.
(iii) Model validation with real ecological data: Applying the model to field observations of specific predator-prey systems and using statistical methods to fit and validate parameters would strengthen the ecological relevance and predictive power of the theoretical framework developed here. Such extensions would not only deepen the theoretical understanding of spatiotemporal dynamics in interacting populations but also enhance the applicability of the model in conservation biology and ecosystem management.

## Appendix

*Appendix A. The calculations of the normal form*

By equation transformation, model (2.3) can be written in the following form

$$\frac{\mathrm{d}U(t)}{\mathrm{d}t} = D(\zeta)(U_t)_{xx} + L(\zeta)U_t + F(U_t, \zeta), \tag{A.1}$$

where $\varphi = (\varphi^{(1)}, \varphi^{(2)})^T \in M$, and each component is represented as follows:

$$D(\zeta)(\varphi)_{xx} = D_0(\varphi)_{xx} + F^d(\varphi, \zeta),$$

where

$$\begin{aligned} D_0(\varphi)_{xx} &= \tau^* \begin{pmatrix} d_{11} + d_{11}d_{12}v^* & d_{11}d_{12}u^* \\ d_{21}d_{22}v^* & d_{22} + d_{21}d_{22}u^* \end{pmatrix} \begin{pmatrix} \varphi^{(1)}_{xx}(0) \\ \varphi^{(2)}_{xx}(0) \end{pmatrix} \\ &= \tau^* B_1 \varphi_{xx}(0), \end{aligned}$$

$$\begin{aligned} F^d(\varphi, \zeta) =& (\tau^* + \zeta) \begin{pmatrix} d_{11}d_{12}\varphi^{(2)}(0)\varphi^{(1)}_{xx}(0) + 2d_{11}d_{12}\varphi^{(1)}_{x}(0)\varphi^{(2)}_{x}(0) + d_{11}d_{12}\varphi^{(1)}(0)\varphi^{(2)}_{xx}(0) \\ d_{21}d_{22}\varphi^{(1)}(0)\varphi^{(2)}_{xx}(0) + 2d_{21}d_{22}\varphi^{(1)}_{x}(0)\varphi^{(2)}_{x}(0) + d_{21}d_{22}\varphi^{(2)}(0)\varphi^{(1)}_{xx}(0) \end{pmatrix} \\ &+ \zeta \begin{pmatrix} (d_{11} + d_{11}d_{12}v^*)\varphi^{(1)}_{xx}(0) + d_{11}d_{12}u^*\varphi^{(2)}_{xx}(0) \\ d_{21}d_{22}v^*\varphi^{(1)}_{xx}(0) + (d_{22} + d_{21}d_{22}u^*)\varphi^{(2)}_{xx}(0) \end{pmatrix}, \end{aligned} \tag{A.2}$$

and

$$\begin{aligned} L(\zeta)(\varphi) &= (\tau^* + \zeta)\left( \begin{pmatrix} \alpha_{11} & \alpha_{12} \\ 0 & 0 \end{pmatrix} \begin{pmatrix} \varphi^{(1)}(0) \\ \varphi^{(2)}(0) \end{pmatrix} + \begin{pmatrix} \beta_{11} & 0 \\ 0 & 0 \end{pmatrix} \begin{pmatrix} \varphi^{(1)}(-1) \\ \varphi^{(2)}(-1) \end{pmatrix} + \begin{pmatrix} 0 & 0 \\ \beta_{21} & \beta_{22} \end{pmatrix} \begin{pmatrix} \varphi^{(1)}(-\frac{\tau_2}{\tau^*+\zeta}) \\ \varphi^{(2)}(-\frac{\tau_2}{\tau^*+\zeta}) \end{pmatrix} \right) \\ &= (\tau^* + \zeta)\left( A_1\varphi(0) + A_2\varphi(-1) + A_3\varphi(-\frac{\tau_2}{\tau^* + \zeta}) \right), \end{aligned}$$

$$F(\varphi, \zeta) = (\tau^* + \zeta) \begin{pmatrix} f\left(\varphi^{(1)}(0) + u^*, \varphi^{(2)}(0) + v^*, \varphi^{(1)}(-1) + u^*\right) \\ g\left(\varphi^{(2)}(0) + v^*, \varphi^{(1)}(-\frac{\tau_2}{\tau^*+\zeta}) + u^*, \varphi^{(2)}(-\frac{\tau_2}{\tau^*+\zeta}) + v^*\right) \end{pmatrix} - L(\zeta)(\varphi). \tag{A.3}$$

Based on the previous expression, by separating the linear term from the nonlinear term, we can rewrite Eq (A.1) as

$$\frac{\mathrm{d}U(t)}{\mathrm{d}t} = D_0(U_t)_{xx} + L_0(U_t) + \tilde{F}(U_t, \zeta), \tag{A.4}$$

where

$$\begin{aligned} L_0(\varphi) &= \tau^* \left( A_1\varphi(0) + A_2\varphi(-1) + A_3\varphi(-\frac{\tau_2}{\tau^*}) \right), \\ \tilde{F}(\varphi, \zeta) &= L(\zeta)(\varphi) - L_0(\varphi) + F(\varphi, \zeta) + F^d(\varphi, \zeta). \end{aligned} \tag{A.5}$$

From the previous statement, the linear system of Eq (A.4) is represented as follows

$$\frac{\mathrm{d}U(t)}{\mathrm{d}t} = D_0(U_t)_{xx} + L_0(U_t). \tag{A.6}$$

According to [35], in order to write Eq (A.4) as an abstract ordinary differential equation in Banach space, we choose the following amplification space:

$$C := \left\{ \Phi \middle| \Phi \in C([-\max\{1, \frac{\tau_2}{\tau_1}\}, 0], X), \exists \lim_{\kappa \to 0^-} \Phi(\kappa) \in X \right\}.$$

Then, Eq (A.4) is equivalent to an abstract ordinary differential equation on $C$

$$\frac{\mathrm{d}U_t}{\mathrm{d}t} = \tilde{H}U_t + Z_0\tilde{F}(U_t, \zeta). \tag{A.7}$$

where $\tilde{H}$ is a linear operator from $M_0^1 = \left\{ \varphi \in M \middle| \dot{\varphi} \in M, \varphi(0) \in \mathrm{dom}((\cdot)_{xx}) \right\}$ to $C$, and there are the following statements:

$$\tilde{H}\varphi = \dot{\varphi} + Z_0\left(\tau^* B_1\varphi_{xx}(0) + L_0(\varphi) - \dot{\varphi}(0)\right),$$

and $Z_0 = Z_0(\kappa)$ is expressed as follows:

$$Z_0(\kappa) = \begin{cases} 0, \kappa \in [-\max\{1, \frac{\tau_2}{\tau_1}\}, 0), \\ 1, \kappa = 0. \end{cases}$$

Next, we use the method proposed in [44] to decompose $C$. Let

$$M_2 := C([-\max\{1, \frac{\tau_2}{\tau_1}\}, 0]; \mathbb{R}^2),\ M_2^* := C([0, \max\{1, \frac{\tau_2}{\tau_1}\}]; \mathbb{R}^{2*}),$$

where $\mathbb{R}^{2*}$ is the two-dimensional space of row vector. The adjoint bilinear form on $M_2^* \times M_2$ is defined as follows:

$$\langle \mathcal{P}(s), \mathcal{Q}(\kappa) \rangle = \mathcal{P}(0)\mathcal{Q}(0) - \int_{-\max\{1, \frac{\tau_2}{\tau_1}\}}^{0} \int_{\xi=0}^{\kappa} \mathcal{P}(\xi - \kappa)\mathrm{d}\mathcal{W}_n(\kappa)\mathcal{Q}(\xi)\mathrm{d}\xi,$$

where $\mathcal{P} \in M_2^*$, $\mathcal{Q} \in M_2$, and $\mathcal{W}_n(\kappa) \in BV\left([-\max\{1, \frac{\tau_2}{\tau_1}\}, 0]; \mathbb{R}^{2\times 2}\right)$, such that for $\mathcal{Q}(\kappa) \in M_2$, and we have

$$-\tau^*(\frac{n_s}{l})^2 B_1\mathcal{Q}_{xx}(0) + L_0\left(\mathcal{Q}(\kappa)\right) = \int_{-\max\{1, \frac{\tau_2}{\tau_1}\}}^{0} \mathrm{d}\mathcal{W}_n(\kappa)\mathcal{Q}(\kappa),$$

where $\mathcal{Q}(\kappa) = (q(\kappa), \bar{q}(\kappa))$ and $\mathcal{P}(s) = \left(p(s)^T, \bar{p}(s)^T\right)^T$; $q(\kappa) = (q_1(\kappa), q_2(\kappa))^T = qe^{i\omega\tau^*\kappa}$ and $p(s) = (p_1(s), p_2(s))^T = pe^{-i\omega\tau^* s}$; $q = (q_1, q_2)$ is the eigenvector corresponding to the eigenvalues $i\omega\tau^*$ of Eq (A.6); and $p = (p_1, p_2)^T$ is the adjoint eigenvector corresponding to the eigenvalues $-i\omega\tau^*$ of Eq (A.6). They meet the following condition

$$\langle \mathcal{P}(s), \mathcal{Q}(\kappa) \rangle = I_2.$$

Through calculation, we obtain

$$q = \left( \frac{1}{\dfrac{\beta_{21}e^{-i\omega\tau_2} - (\frac{n_s}{l})^2 d_{21}d_{22}v^*}{(d_{22} + d_{21}d_{22}u^*)(\frac{n_s}{l})^2 - \beta_{22}e^{-i\omega\tau_2} + i\omega}} \right),\ p = \eta \left( \frac{1}{\dfrac{\alpha_{12} - (\frac{n_s}{l})^2 d_{11}d_{12}u^*}{(d_{22} + d_{21}d_{22}u^*)(\frac{n_s}{l})^2 - \beta_{22}e^{-i\omega\tau_2} + i\omega}} \right),$$

where

$$\eta = \frac{k_1^2}{(1+\beta_{11}\tau^* e^{-i\omega\tau^*})k_1^2 + (1+\beta_{22}\tau_2 e^{-i\omega\tau_2})k_2 + k_1\beta_{21}\alpha_{12}\tau_2 e^{-i\omega\tau_2} - (\frac{n_s}{l})^2 k_1\beta_{21}d_{11}d_{12}u^*\tau_2 e^{-i\omega\tau_2}},$$

$$k_1 = (d_{22} + d_{21}d_{22}u^*)(\frac{n_s}{l})^2 - \beta_{22}e^{-i\omega\tau_2} + i\omega,$$

$$k_2 = \alpha_{12}\beta_{21}e^{-i\omega\tau_2} - \alpha_{12}(\frac{n_s}{l})^2 d_{21}d_{22}v^* - (\frac{n_s}{l})^2 d_{11}d_{12}u^*\beta_{21}e^{-i\omega\tau_2} + (\frac{n_s}{l})^4 d_{11}d_{12}d_{21}d_{22}u^*v^*.$$

According to [35, 42, 44], phase space $C$ can be decomposed into

$$C = \mathrm{Im}\pi \oplus \mathrm{Ker}\pi,$$

where $\pi : C \longrightarrow \mathrm{Im}\pi$. For $\psi \in M$, we have

$$\pi(\psi) = \left(\mathcal{Q}(\kappa)\left\langle \mathcal{P}(0), \begin{pmatrix}[\psi(\cdot), \beta_{n_s}^{(1)}] \\ [\psi(\cdot), \beta_{n_s}^{(2)}]\end{pmatrix}\right\rangle\right)^T b_{n_s}(x). \tag{A.8}$$

Through the above analysis, we decompose $U_t(\kappa)$ into

$$\begin{aligned} U_t(\kappa) &= \left(\mathcal{Q}(\kappa)\begin{pmatrix} m_1 \\ m_2\end{pmatrix}\right)^T \begin{pmatrix}\beta_{n_s}^{(1)} \\ \beta_{n_s}^{(2)}\end{pmatrix} + z \\ &= \left(m_1 q e^{i\omega\tau^*\kappa} + m_2\bar{q}e^{-i\omega\tau^*\kappa}\right) b_{n_s}(x) + \begin{pmatrix} z^{(1)} \\ z^{(2)}\end{pmatrix} \\ &= \mathcal{Q}(\kappa)m_x + z, \end{aligned}$$

where $z \in \mathcal{P}^1 := M_0^1 \cap \mathrm{Ker}\pi$, $m_x = (m_1 b_n(x), m_2 b_n(x))^T$ and $z = \left(z^{(1)}, z^{(2)}\right)^T$. Therefore, we can decompose the system (A.7) into the following abstract ordinary differential equation on $\mathbb{R}^2 \times \mathrm{Ker}\pi$

$$\begin{cases} \dot{m} = \mathcal{V}m + \mathcal{P}(0)\begin{pmatrix}[\tilde{F}(\mathcal{Q}(\kappa)m_x + z, \zeta), \beta_{n_s}^{(1)}] \\ [\tilde{F}(\mathcal{Q}(\kappa)m_x + z, \zeta), \beta_{n_s}^{(2)}]\end{pmatrix}, \\ \dot{z} = \mathcal{A}_{\mathcal{P}^1} z + (I - \pi)Z_0(\kappa)\tilde{F}(\mathcal{Q}(\kappa)m_x + z, \zeta), \end{cases} \tag{A.9}$$

where $m = (m_1, m_2)^T$, $\mathcal{V} = \mathrm{diag}\{i\omega\tau^*, -i\omega\tau^*\}$, and $\mathcal{A}_{\mathcal{P}^1} : \mathcal{P}^1 \longrightarrow \mathrm{Ker}\pi$ are represented by

$$\mathcal{A}_{\mathcal{P}^1} z = \dot{z} + Z_0(\kappa)\left(\tau^* B_1 z_{xx}(0) + L_0(z) - \dot{z}(0)\right).$$

Next, we consider the following Taylor expansions

$$\begin{aligned} L(\zeta)(\varphi) &= \sum_{i\geq 1}\frac{1}{i!}L_i(\zeta)(\varphi), \quad \tilde{F}(\varphi, \zeta) = \sum_{i\geq 2}\frac{1}{i!}\tilde{F}_i(\varphi, \zeta), \\ F(\varphi, \zeta) &= \sum_{i\geq 2}\frac{1}{i!}F_i(\varphi, \zeta), \quad F^d(\varphi, \zeta) = \sum_{i\geq 2}\frac{1}{i!}F_i^d(\varphi, \zeta). \end{aligned}$$

Combining Eq (A.5), we have

$$\tilde{F}_2(\varphi, \zeta) = 2\zeta\left(A_1\varphi(0) + A_2\varphi(-1) + A_3\varphi(-\frac{\tau_2}{\tau^*}) + \frac{\tau_2}{\tau^*}A_3\varphi'(-\frac{\tau_2}{\tau^*})\right) + F_2(\varphi, \zeta) + F_2^d(\varphi, \zeta), \tag{A.10}$$

and

$$\tilde{F}_i(\varphi,\zeta) = L_i(\zeta)(\varphi) + F_i(\varphi,\zeta) + F_i^d(\varphi,\zeta), i = 3, 4\cdots. \tag{A.11}$$

Therefore, Eq (A.9) can be rewritten as

$$\begin{cases} \dot{m} = \mathcal{V}m + \sum\limits_{i\geq 2}\dfrac{1}{i!}f_i^1(m,z,\zeta), \\ \dot{z} = \mathcal{A}_{\mathcal{P}^1}z + \sum\limits_{i\geq 2}\dfrac{1}{i!}f_i^2(m,z,\zeta), \end{cases} \tag{A.12}$$

where

$$\begin{cases} f_i^1(m,z,\zeta) = \mathcal{P}(0)\left(\begin{bmatrix}\tilde{F}_i(Q(\kappa)m_x + z,\zeta),\beta_{n_s}^{(1)}\\ \tilde{F}_i(Q(\kappa)m_x + z,\zeta),\beta_{n_s}^{(2)}\end{bmatrix}\right), \\ f_i^2(m,z,\zeta) = (I-\pi)Z_0(\kappa)\tilde{F}_i(Q(\kappa)m_x + z,\zeta). \end{cases} \tag{A.13}$$

According to the normal form theory of partial functional differential equations [44], by applying the following variable transformations

$$(m,z) = (\tilde{m},\tilde{z}) + \frac{1}{i!}\left(U_i^1(\tilde{m},\zeta), U_i^2(\tilde{m},\zeta)\right), i \geq 2, \tag{A.14}$$

where $m,\tilde{m}\in\mathbb{R}^2$, $z,\tilde{z}\in\mathcal{P}^1$, $U_i^1:\mathbb{R}^3\to\mathbb{R}^2$ and $U_i^2:\mathbb{R}^3\to\mathcal{P}^1$ are homogeneous polynomials of degree $i$ in $\tilde{m}$ and $\zeta$, we obtain the normal form of (A.12), as follows:

$$\dot{m} = \mathcal{V}m + \sum_{i\geq 2} g_i^1(m,0,\zeta).$$

According to [35, 41, 42], by defining $\left(M_i^1 q\right)(m,\zeta) = \mathcal{D}_m q(m,\zeta)\mathcal{V}m - \mathcal{V}q(m,\zeta)$ and $\left(M_i^2 h\right)(m,\zeta) = \mathcal{D}_m h(m,\zeta)\mathcal{V}m - \mathcal{A}_{\mathcal{P}^1}h(m,\zeta)$, we have

$$g_2^1(m,0,\zeta) = \mathrm{Proj}_{\mathrm{Ker}(M_2^1)}f_2^1(m,0,\zeta), \tag{A.15}$$

and

$$g_3^1(m,0,\zeta) = \mathrm{Proj}_{\mathrm{Ker}(M_3^1)}\tilde{f}_3^1(m,0,\zeta) = \mathrm{Proj}_S\tilde{f}_3^1(m,0,0) + O\left(\zeta^2|m|\right), \tag{A.16}$$

where $\tilde{f}_3^1(m,0,\zeta)$ is the cubic polynomial of $(m,\zeta)$ under the variable transformation of (A.14), and it can be determined by Eq (A.16),

$$\ker(M_2^1) = \mathrm{Span}\left\{\begin{pmatrix}\zeta m_1\\0\end{pmatrix},\begin{pmatrix}0\\\zeta m_2\end{pmatrix}\right\},$$

$$\ker(M_3^1) = \mathrm{Span}\left\{\begin{pmatrix}m_1^2m_2\\0\end{pmatrix},\begin{pmatrix}\zeta^2m_1\\0\end{pmatrix},\begin{pmatrix}0\\m_1m_2^2\end{pmatrix},\begin{pmatrix}0\\\zeta^2m_2\end{pmatrix}\right\},$$

and

$$S = \mathrm{Span}\left\{\begin{pmatrix}m_1^2m_2\\0\end{pmatrix},\begin{pmatrix}0\\m_1m_2^2\end{pmatrix}\right\}. \tag{A.17}$$

For the convenience of representing subsequent calculations, denote

$$\mathcal{B}(\alpha m_1^{u_1}m_2^{u_2}\zeta) = \begin{pmatrix}\alpha m_1^{u_1}m_2^{u_2}\zeta\\ \bar{\alpha}m_1^{u_2}m_2^{u_1}\zeta\end{pmatrix}, \alpha\in\mathbb{C}.$$

Calculation of $g_2^1(m,,0,\zeta)$

According to Eq (A.2), we have

$$F_2^d(\varphi,\zeta) = F_{20}^d(\varphi) + \zeta F_{21}^d(\varphi) \tag{A.18}$$

and

$$F_3^d(\varphi,\zeta) = \zeta F_{31}^d(\varphi),\ F_i^d(\varphi,\zeta) = (0,0)^T,\ i = 4,5\cdots, \tag{A.19}$$

where

$$\begin{cases} F_{20}^d(\varphi) = 2\tau^* \begin{pmatrix} d_{11}d_{12}\varphi^{(2)}(0)\varphi_{xx}^{(1)}(0) + 2d_{11}d_{12}\varphi_x^{(1)}(0)\varphi_x^{(2)}(0) + d_{11}d_{12}\varphi^{(1)}(0)\varphi_{xx}^{(2)}(0) \\ d_{21}d_{22}\varphi^{(1)}(0)\varphi_{xx}^{(2)}(0) + 2d_{21}d_{22}\varphi_x^{(1)}(0)\varphi_x^{(2)}(0) + d_{21}d_{22}\varphi^{(2)}(0)\varphi_{xx}^{(1)}(0) \end{pmatrix}, \\ F_{21}^d(\varphi) = 2B_1\varphi_{xx}(0), \\ F_{31}^d(\varphi) = 6 \begin{pmatrix} d_{11}d_{12}\varphi^{(2)}(0)\varphi_{xx}^{(1)}(0) + 2d_{11}d_{12}\varphi_x^{(1)}(0)\varphi_x^{(2)}(0) + d_{11}d_{12}\varphi^{(1)}(0)\varphi_{xx}^{(2)}(0) \\ d_{21}d_{22}\varphi^{(1)}(0)\varphi_{xx}^{(2)}(0) + 2d_{21}d_{22}\varphi_x^{(1)}(0)\varphi_x^{(2)}(0) + d_{21}d_{22}\varphi^{(2)}(0)\varphi_{xx}^{(1)}(0) \end{pmatrix}. \end{cases} \tag{A.20}$$

Therefore, we can obtain

$$\begin{aligned} &\left( \begin{bmatrix} 2\zeta \left( A_1 \left( Q(0)m_x \right) + A_2 \left( Q(-1)m_x \right) + A_3 \left( Q(-\frac{\tau_2}{\tau^*})m_x \right) + \frac{\tau_2}{\tau^*} A_3 \left( Q'(-\frac{\tau_2}{\tau^*})m_x \right) \right),\ \beta_{n_s}^{(1)} \\ 2\zeta \left( A_1 \left( Q(0)m_x \right) + A_2 \left( Q(-1)m_x \right) + A_3 \left( Q(-\frac{\tau_2}{\tau^*})m_x \right) + \frac{\tau_2}{\tau^*} A_3 \left( Q'(-\frac{\tau_2}{\tau^*})m_x \right) \right),\ \beta_{n_s}^{(2)} \end{bmatrix} \right) \\ &= 2\zeta \left( A_1 Q(0) + A_2 Q(-1) + (1 + i\omega\tau_2) A_3 Q(-\tfrac{\tau_2}{\tau^*}) \right) \begin{pmatrix} m_1 \\ m_2 \end{pmatrix}, \end{aligned} \tag{A.21}$$

and

$$\left( \begin{bmatrix} \zeta F_{21}^d \left( Q(\kappa)m_x \right), \beta_{n_s}^{(1)} \\ \zeta F_{21}^d \left( Q(\kappa)m_x \right), \beta_{n_s}^{(2)} \end{bmatrix} \right) = -2 \left( \frac{n_s}{l} \right)^2 \zeta \left( B_1 \left( Q(0) \begin{pmatrix} m_1 \\ m_2 \end{pmatrix} \right) \right). \tag{A.22}$$

Besides, for all $\zeta \in \mathbb{R}$, we have $F_2\left(Q(\kappa)m_x, \zeta\right) = F_2\left(Q(\kappa)m_x, 0\right)$. From the first expression of Eq (A.13), we can obtain

$$f_2^1(m,0,\zeta) = \mathcal{P}(0) \left( \begin{bmatrix} \tilde{F}_2(Q(\kappa)m_x,\ \zeta),\ \beta_{n_s}^{(1)} \\ \tilde{F}_2(Q(\kappa)m_x,\ \zeta),\ \beta_{n_s}^{(2)} \end{bmatrix} \right). \tag{A.23}$$

Combining Eqs (A.18)–(A.23), we get

$$g_2^1(m,0,\zeta) = \mathrm{Proj}_{\ker(M_2^1)} f_2^1(m,0,\zeta) = \mathcal{B}(N_1\zeta m_1), \tag{A.24}$$

where

$$N_1 = 2p^T \left( A_1 q(0) + A_2 q(-1) + (1 + i\omega\tau_2) A_3 q(-\frac{\tau_2}{\tau^*}) - \left( \frac{n_s}{l} \right)^2 B_1 q(0) \right).$$

Calculation of $g_3^1(m,,0,\zeta)$

We need to calculate $g_3^1(m,,0,\zeta)$ from Eq (A.16). Denote

$$f_2^{(1,1)}(m,z,0) = \mathcal{P}(0) \left( \begin{bmatrix} F_2(Q(\kappa)m_x + z, 0), \beta_{n_s}^{(1)} \\ F_2(Q(\kappa)m_x + z, 0), \beta_{n_s}^{(2)} \end{bmatrix} \right), \tag{A.25}$$

$$f_2^{(1,2)}(m,z,0) = \mathcal{P}(0)\left(\begin{bmatrix} F_2^d(\mathcal{Q}(\kappa)m_x + z, 0), \beta_{n_s}^{(1)} \\ F_2^d(\mathcal{Q}(\kappa)m_x + z, 0), \beta_{n_s}^{(2)} \end{bmatrix}\right). \tag{A.26}$$

According to Eq (A.24), we can obtain $g_2^1(m,0,0) = (0,0)^T$. Then, $\tilde{f}_3^1(m,0,0)$ is expressed by the following formula

$$\begin{aligned}\tilde{f}_3^1(m,0,0) =& f_3^1(m,0,0) + \frac{3}{2}\left[\left(\mathcal{D}_m f_2^1(m,0,0)\mathcal{V}_2^1(m,0) + \left(\mathcal{D}_z f_2^{(1,1)}(m,0,0)\right)\mathcal{V}_2^2(m,0)(\kappa)\right)\right] \\ &+ \frac{3}{2}\left[\left(\mathcal{D}_{z,z_x,z_{xx}} f_2^{(1,2)}(m,0,0)\mathcal{V}_2^{(2,d)}(m,0)(\kappa)\right)\right],\end{aligned}$$

where

$$f_2^1(m,0,0) = f_2^{(1,1)}(m,0,0) + f_2^{(1,2)}(m,0,0), \tag{A.27}$$

$$\mathcal{V}_2^1(m,0) = \left(M_2^1\right)^{-1}\mathrm{Proj}_{\mathrm{Im}(M_2^1)} f_2^1(m,0,0),\ \mathcal{V}_2^2(m,0) = \left(M_2^2\right)^{-1} f_2^2(m,0,0), \tag{A.28}$$

$$\mathcal{D}_{z,z_x,z_{xx}} f_2^{(1,2)}(m,0,0) = \left(\mathcal{D}_z f_2^{(1,2)}(m,0,0), \mathcal{D}_{z_x} f_2^{(1,1)}(m,0,0), \mathcal{D}_{z_{xx}} f_2^{(1,2)}(m,0,0)\right), \tag{A.29}$$

$$\mathcal{V}_2^{(2,d)}(m,0)(\kappa) = \left(\mathcal{V}_2^2(m,0)(\kappa), \mathcal{V}_{2x}^2(m,0)(\kappa), \mathcal{V}_{2xx}^2(m,0)(\kappa)\right)^T. \tag{A.30}$$

Next, we divide it into the following four steps to calculate $\mathrm{Proj}_S \tilde{f}_3^1(m,0,0)$.

**Step 1**. The calculation of $\mathrm{Proj}_S f_3^1(m,0,0)$.

Let

$$F_3(\mathcal{Q}(\kappa)m_x, 0) = \sum_{u_1+u_2=3} \Phi_{u_1u_2} m_1^{u_1} m_2^{u_2} b_{n_s}^3(x),\ u_1,\ u_2 \in \mathrm{N}_0. \tag{A.31}$$

From Eqs (A.11) and (A.19), we obtain $\tilde{F}_3(\mathcal{Q}(\kappa)m_x, 0) = F_3(\mathcal{Q}(\kappa)m_x, 0)$, and it can be inferred from Eqs (A.13) and (A.31) that

$$f_3^1(m,0,0) = \mathcal{P}(0)\left(\sum_{u_1+u_2=3} \Phi_{u_1u_2} m_1^{u_1} m_2^{u_2} \int_0^{l\pi} b_{n_s}^4(x)\mathrm{d}x\right),$$

where $\int_0^{l\pi} b_{n_s}^4(x)\mathrm{d}x = \frac{3}{2l\pi}$, and then we have

$$\mathrm{Proj}_S f_3^1(m,0,0) = \mathcal{B}(N_{21} m_1^2 m_2),$$

where

$$N_{21} = \frac{3}{2l\pi} p^T \Phi_{21}.$$

**Step 2**. The calculation of $\mathrm{Proj}_S\left(\mathcal{D}_m f_2^1(m,0,0)\mathcal{V}_2^1(m,0)\right)$.

According to Eqs (A.10) and (A.18), we have

$$\tilde{F}_2(\mathcal{Q}(\kappa)m_x,\ 0) = F_2(\mathcal{Q}(\kappa)m_x,\ 0) + F_{20}^d(\mathcal{Q}(\kappa)m_x). \tag{A.32}$$

From Eq (A.3), we have

$$\begin{aligned}F_2\left(\mathcal{Q}(\kappa)m_x + z,\ \zeta\right) &= F_2\left(\mathcal{Q}(\kappa)m_x + z,\ 0\right) \\ &= b_{n_s}^2(x)\left(\sum_{u_1+u_2=2} \Phi_{u_1u_2} m_1^{u_1} m_2^{u_2}\right) + \mathcal{S}_2\left(\mathcal{Q}(\kappa)m_x,\ z\right) + O\left(|z|^2\right),\end{aligned} \tag{A.33}$$

where $\mathcal{S}_2\left(Q(\kappa)m_x,\ z\right)$ represents the product of $Q(\kappa)m_x$ and $z$. From Eqs (A.18) and (A.20), we have

$$F_2^d\left(Q(\kappa)m_x, 0\right) = F_{20}^d\left(Q(\kappa)m_x\right) = \left(\frac{n_s}{l}\right)^2 \left(\rho_{n_s}^2(x) - b_{n_s}^2(x)\right)\left(\sum_{u_1+u_2=2} \Phi_{u_1u_2}^d m_1^{u_1} m_2^{u_2}\right), \tag{A.34}$$

where

$$\rho_{n_s}(x) = \frac{\sqrt{2}}{\sqrt{l\pi}} \sin\left(\frac{n_s x}{l}\right),$$

$$\begin{cases} \Phi_{20}^d = 2q_1(0)q_2(0)\tau^* \begin{pmatrix} d_{11}d_{12} \\ d_{21}d_{22} \end{pmatrix} = \overline{\Phi_{02}^d}, \\ \Phi_{11}^d = 2\tau^* \begin{pmatrix} 4d_{11}d_{12}Re\left\{\overline{q}_1(0)q_2(0)\right\} \\ 4d_{21}d_{22}Re\left\{q_1(0)\overline{q}_2(0)\right\} \end{pmatrix}. \end{cases} \tag{A.35}$$

Noted that $\int_0^{l\pi} \rho_{n_s}^2(x) b_{n_s}(x)\mathrm{d}x = \int_0^{l\pi} b_{n_s}^3(x)\mathrm{d}x = 0$. Based on the previous content, we have

$$f_2^1(m, 0, 0) = \mathcal{P}(0)\left(\begin{bmatrix} \tilde{F}_2(Q(\kappa)m_x,\ 0),\ \beta_{n_s}^{(1)} \\ \tilde{F}_2(Q(\kappa)m_x,\ 0),\ \beta_{n_s}^{(2)} \end{bmatrix}\right) = (0, 0)^T. \tag{A.36}$$

By combining (A.18) and (A.36), we have

$$\mathrm{Proj}_S\left(\mathcal{D}_m f_2^1(m, 0, 0)\mathcal{V}_2^1(m, 0)\right) = \mathcal{B}(N_{22}m_1^2 m_2),$$

where

$$N_{22} = (0, 0)^T.$$

**Step 3**. The calculation of $\mathrm{Proj}_S\left(\left(\mathcal{D}_z f_2^{(1,1)}(m, 0, 0)\right)\mathcal{V}_2^2(m, 0)(\kappa)\right)$.

Let

$$\mathcal{V}_2^2(m, 0)(\kappa) = h(\kappa, m) = \sum_{n\in \mathrm{N}_0} h_n(\kappa, m) b_n(x), \tag{A.37}$$

where

$$h_n(\kappa, m) = \sum_{u_1+u_2=2} h_{n,u_1u_2}(\kappa) m_1^{u_1} m_2^{u_2}.$$

Therefore, we can directly obtain

$$\left(\begin{bmatrix} \mathcal{S}_2\left(Q(\kappa)m_x,\ \sum\limits_{n\in \mathrm{N}_0} h_n(\kappa, m)b_n(x)\right),\ \beta_{n_s}^{(1)} \\ \mathcal{S}_2\left(Q(\kappa)m_x,\ \sum\limits_{n\in \mathrm{N}_0} h_n(\kappa, m)b_n(x)\right),\ \beta_{n_s}^{(2)} \end{bmatrix}\right) = \sum_{n\in \mathrm{N}_0} \mathcal{Z}_n \left(\mathcal{S}_2(q(\kappa)m_1, h_n(\kappa, m)) + \mathcal{S}_2(\bar{q}(\kappa)m_2, h_n(\kappa, m))\right),$$

where

$$\mathcal{Z}_n = \int_0^{l\pi} b_{n_s}^2(x) b_n(x)\mathrm{d}x = \begin{cases} \dfrac{1}{\sqrt{l\pi}},\ n = 0, \\ \dfrac{1}{\sqrt{2l\pi}},\ n = 2n_s, \\ 0,\ otherwise. \end{cases}$$

Therefore, we have

$$\left(\mathcal{D}_z f_2^{(1,1)}(m,0,0)\right)\mathcal{V}_2^2(m,0)(\kappa) = \mathcal{P}(0)\left(\sum_{n=0,2n_s}\mathcal{Z}_n\left(\mathcal{S}_2(q(\kappa)m_1, h_n(\kappa,m)) + \mathcal{S}_2(\bar{q}(\kappa)m_2, h_n(\kappa,m))\right)\right),$$

$$\mathrm{Proj}_S\left(\left(\mathcal{D}_z f_2^{(1,1)}(m,0,0)\right)\mathcal{V}_2^2(m,0)(\kappa)\right) = \mathcal{B}(N_{23}m_1^2m_2),$$

where

$$N_{23} = \frac{1}{\sqrt{l\pi}}p^T\left(\mathcal{S}_2(q(\kappa),\ h_{0,11}(\kappa)) + \mathcal{S}_2(\bar{q}(\kappa),\ h_{0,20}(\kappa))\right) + \frac{1}{\sqrt{2l\pi}}p^T\left(\mathcal{S}_2(q(\kappa),\ h_{2n_s,11}(\kappa)) + \mathcal{S}_2(\bar{q}(\kappa),\ h_{2n_s,20}(\kappa))\right).$$

**Step 4**. The calculation of $\mathrm{Proj}_S\left(\left(\mathcal{D}_{z,z_x,z_{xx}} f_2^{(1,2)}(m,0,0)\right)\mathcal{V}_2^{(2,d)}(m,0)(\kappa)\right)$.

Denote $U(\kappa) = (U^{(1)},\ U^{(2)}) = \mathcal{Q}(\kappa)m_x$ and

$$\begin{aligned}
F_2^d(U(\kappa),\ z,\ z_x,\ z_{xx}) =& F_2^d(U(\kappa)+z,\ 0) = F_{20}^d(U(\kappa)+z)\\
=& 2\tau^*\begin{pmatrix} d_{11}d_{12}\left(U_{xx}^{(1)}(0)+z_{xx}^{(1)}(0)\right)\left(U^{(2)}(0)+z^{(2)}(0)\right)\\ d_{21}d_{22}\left(U_{xx}^{(2)}(0)+z_{xx}^{(2)}(0)\right)\left(U^{(1)}(0)+z^{(1)}(0)\right)\end{pmatrix}\\
&+ 4\tau^*\begin{pmatrix} d_{11}d_{12}\left(U_{x}^{(1)}(0)+z_{x}^{(1)}(0)\right)\left(U_x^{(2)}(0)+z_x^{(2)}(0)\right)\\ d_{21}d_{22}\left(U_{x}^{(2)}(0)+z_{x}^{(2)}(0)\right)\left(U_x^{(1)}(0)+z_x^{(1)}(0)\right)\end{pmatrix}\\
&+ 2\tau^*\begin{pmatrix} d_{11}d_{12}\left(U_{xx}^{(2)}(0)+z_{xx}^{(2)}(0)\right)\left(U^{(1)}(0)+z^{(1)}(0)\right)\\ d_{21}d_{22}\left(U_{xx}^{(1)}(0)+z_{xx}^{(1)}(0)\right)\left(U^{(2)}(0)+z^{(2)}(0)\right)\end{pmatrix}.
\end{aligned}$$

According to [41], we have

$$\begin{cases}
\tilde{\mathcal{S}}_2^{(d,1)}(q(\kappa),\ y(\kappa)) = 2\tau^*\begin{pmatrix} d_{11}d_{12}\left(q_1(0)y_2(0)+q_2(0)y_1(0)\right)\\ d_{21}d_{22}\left(q_2(0)y_1(0)+q_1(0)y_2(0)\right)\end{pmatrix},\\
\tilde{\mathcal{S}}_2^{(d,2)}(q(\kappa),\ y(\kappa)) = 4\tau^*\begin{pmatrix} d_{11}d_{12}\left(q_1(0)y_2(0)+q_2(0)y_1(0)\right)\\ d_{21}d_{22}\left(q_2(0)y_1(0)+q_1(0)y_2(0)\right)\end{pmatrix},\\
\tilde{\mathcal{S}}_2^{(d,3)}(q(\kappa),\ y(\kappa)) = 2\tau^*\begin{pmatrix} d_{11}d_{12}\left(q_1(0)y_2(0)+q_2(0)y_1(0)\right)\\ d_{21}d_{22}\left(q_2(0)y_1(0)+q_1(0)y_2(0)\right)\end{pmatrix}.
\end{cases}$$

From (A.26), (A.30), and (A.37), we have

$$\left(\mathcal{D}_{z,z_x,z_{xx}} f_2^{(1,2)}(m,0,0)\right)\mathcal{V}_2^{(2,d)}(m,0)(\kappa) = \mathcal{P}(0)\left(\begin{bmatrix}\left(\mathcal{D}_{z,z_x,z_{xx}}F_2^d(m,0,0)\right)\mathcal{V}_2^{(2,d)}(m,0)(\kappa),\ \beta_{n_s}^{(1)}\\ \left(\mathcal{D}_{z,z_x,z_{xx}}F_2^d(m,0,0)\right)\mathcal{V}_2^{(2,d)}(m,0)(\kappa),\ \beta_{n_s}^{(2)}\end{bmatrix}\right),$$

therefore, we obtain

$$\mathrm{Proj}_S\left(\left(\mathcal{D}_{z,z_x,z_{xx}} f_2^{(1,2)}(m,0,0)\right)\mathcal{V}_2^{(2,d)}(m,0)(\kappa)\right) = \mathcal{B}(N_{24}m_1^2m_2),$$

where

$$\begin{aligned}
N_{24} =& -\frac{1}{\sqrt{l\pi}}(\frac{n_s}{l})^2 p^T\left(\tilde{\mathcal{S}}_2^{(d,1)}(q(\kappa),\ h_{0,11}(\kappa)) + \tilde{\mathcal{S}}_2^{(d,1)}(\bar{q}(\kappa),\ h_{0,20}(\kappa))\right)\\
&+ \frac{1}{\sqrt{2l\pi}}p^T\sum_{i=1,2,3}c_{2n_s}^{(i)}\left(\tilde{\mathcal{S}}_2^{(d,i)}(q(\kappa),\ h_{2n_s,11}(\kappa)) + \tilde{\mathcal{S}}_2^{(d,i)}(\bar{q}(\kappa),\ h_{2n_s,20}(\kappa))\right)
\end{aligned}$$

and

$$c_{2n_s}^{(1)} = -(\frac{n_s}{l})^2,\ c_{2n_s}^{(2)} = 2(\frac{n_s}{l})^2,\ c_{2n_s}^{(3)} = -4(\frac{n_s}{l})^2.$$

*Appendix B. Calculation of the corresponding coefficients for Theorem 5.1*

**The calculations of $\Phi_{ij}$ and $\mathcal{S}_2\left(\mathcal{Q}(\kappa)m_x, z\right)$**

Denote $\hat{\eta} = \frac{\tau_2}{\tau^*+\zeta}$ and $\bar{\eta} = \frac{\tau_2}{\tau^*}$, we have

$$\begin{aligned} F_2(\varphi, 0) =& f_{200000}\varphi_1^2(0) + f_{020000}\varphi_2^2(0) + f_{000200}\varphi_1^2(-\bar{\eta}) + 2f_{110000}\varphi_1(0)\varphi_2(0) \\ &+ 2f_{101000}\varphi_1(0)\varphi_1(-1) + 2f_{010100}\varphi_2(0)\varphi_1(-\bar{\eta}) \\ &+ 2f_{010010}\varphi_2(0)\varphi_2(-\bar{\eta}) + 2f_{000110}\varphi_1(-\bar{\eta})\varphi_2(-\bar{\eta}), \end{aligned} \tag{B.1}$$

and

$$\begin{aligned} F_3(\varphi, 0) =& f_{300000}\varphi_1^3(0) + f_{030000}\varphi_2^3(0) + f_{000300}\varphi_1^3(-\bar{\eta}) + 3f_{210000}\varphi_1^2(0)\varphi_2(0) \\ &+ 3f_{000210}\varphi_1^2(-\bar{\eta})\varphi_2(-\bar{\eta}) + 3f_{120000}\varphi_1(0)\varphi_2^2(0) \\ &+ 3f_{010200}\varphi_2(0)\varphi_1^2(-\bar{\eta}) + 6f_{010110}\varphi_2(0)\varphi_1(-\bar{\eta})\varphi_2(-\bar{\eta}), \end{aligned} \tag{B.2}$$

where

$$f_{200000} = \begin{pmatrix} \dfrac{2v^*\tau^*(d+ev^*)}{(d+u^*+ev^*)^3} - \tau^* \\ 0 \end{pmatrix}, f_{020000} = \begin{pmatrix} \dfrac{2eu^*\tau^*(d+u^*)}{(d+u^*+ev^*)^3} \\ 0 \end{pmatrix}, f_{000200} = \begin{pmatrix} 0 \\ \dfrac{-2nu^*v^*\tau^*}{(u^*+p)^3} \end{pmatrix},$$

$$f_{110000} = \begin{pmatrix} \dfrac{2ev^*\tau^*(d+ev^*) - \tau^*(d+2ev^*)(d+u^*+ev^*)}{(d+u^*+ev^*)^3} \\ 0 \end{pmatrix}, f_{101000} = \begin{pmatrix} -\tau^* \\ 0 \end{pmatrix}, f_{010100} = \begin{pmatrix} 0 \\ \dfrac{nv^*\tau^*}{(u^*+p)^2} \end{pmatrix},$$

$$f_{010010} = \begin{pmatrix} 0 \\ -\dfrac{n\tau^*}{u^*+p} \end{pmatrix}, f_{000110} = \begin{pmatrix} 0 \\ \dfrac{nv^*\tau^*}{(u^*+p)^2} \end{pmatrix}, f_{300000} = \begin{pmatrix} \dfrac{-6v^*\tau^*(d+ev^*)}{(d+u^*+ev^*)^4} \\ 0 \end{pmatrix}, f_{030000} = \begin{pmatrix} \dfrac{-6e^2u^*\tau^*(d+u^*)}{(d+u^*+ev^*)^4} \\ 0 \end{pmatrix},$$

$$f_{000300} = \begin{pmatrix} 0 \\ \dfrac{6n\tau^*v^{*2}}{(u^*+p)^4} \end{pmatrix}, f_{210000} = \begin{pmatrix} \dfrac{-6ev^*\tau^*(d+ev^*) + 2\tau^*(d+u^*+ev^*)^2}{(d+u^*+ev^*)^4} \\ 0 \end{pmatrix}, f_{000210} = \begin{pmatrix} 0 \\ \dfrac{-2nv^*\tau^*}{(u^*+p)^3} \end{pmatrix},$$

$$f_{120000} = \begin{pmatrix} \dfrac{2e\tau^*(d+u^*+ev^*)^2 - 2e^2v^*\tau^*(d+ev^*) - 4d\tau^*(d+u^*+ev^*) + 8e\tau^*v^*u^*}{(d+u^*+ev^*)^4} \\ 0 \end{pmatrix},$$

$$f_{010200} = \begin{pmatrix} 0 \\ \dfrac{-2nv^*\tau^*}{(u^*+p)^3} \end{pmatrix}, f_{010110} = \begin{pmatrix} 0 \\ \dfrac{n\tau^*}{(u^*+p)^2} \end{pmatrix}.$$

Denote

$$\begin{aligned} \varphi(\kappa) =& \mathcal{Q}(\kappa)m_x = q(\kappa)m_1(t)b_{n_s}(x) + \bar{q}(\kappa)m_2(t)b_{n_s}(x) \\ =& \begin{pmatrix} q_1(\kappa)m_1(t)b_{n_s}(x) + \bar{q}_1(\kappa)m_2(t)b_{n_s}(x) \\ q_2(\kappa)m_1(t)b_{n_s}(x) + \bar{q}_2(\kappa)m_2(t)b_{n_s}(x) \end{pmatrix} \\ =& \begin{pmatrix} \varphi_1(\kappa) \\ \varphi_2(\kappa) \end{pmatrix}. \end{aligned} \tag{B.3}$$

Similar to the expression in (A.31), we have

$$F_2(\mathcal{Q}(\kappa)m_x, 0) = \sum_{u_1+u_2=2} \Phi_{u_1u_2} m_1^{u_1} m_2^{u_2} b_{n_s}^2(x),\ u_1, u_2 \in \mathrm{N}_0. \tag{B.4}$$

By combining equations (A.31) and (B.1)–(B.4), we can calculate that

$$\begin{aligned}
\Phi_{20} =& f_{200000}q_1^2(0) + f_{020000}q_2^2(0) + f_{000200}q_1^2(-\bar{\eta}) + 2f_{110000}q_1(0)q_2(0) + 2f_{101000}q_1(0)q_1(-1)\\
&+ 2f_{010100}q_2(0)q_1(-\bar{\eta}) + 2f_{010010}q_2(0)q_2(-\bar{\eta}) + 2f_{000110}q_1(-\bar{\eta})q_2(-\bar{\eta}),\\
\Phi_{11} =& 2f_{200000}q_1(0)\bar{q}_1(0) + 2f_{020000}q_2(0)\bar{q}_2(0) + 2f_{000200}q_1(-\bar{\eta})\bar{q}_1(-\bar{\eta}) + 2f_{110000}q_1(0)\bar{q}_2(0)\\
&+ 2f_{110000}\bar{q}_1(0)q_2(0) + 2f_{101000}q_1(0)\bar{q}_1(-1) + 2f_{101000}\bar{q}_1(0)q_1(-1)\\
&+ 2f_{010100}q_2(0)\bar{q}_1(-\bar{\eta}) + 2f_{010100}\bar{q}_2(0)q_1(-\bar{\eta}) + 2f_{010010}q_2(0)\bar{q}_2(-\bar{\eta})\\
&+ 2f_{010010}\bar{q}_2(0)q_2(-\bar{\eta}) + 2f_{000110}q_1(-\bar{\eta})\bar{q}_2(-\bar{\eta}) + 2f_{000110}\bar{q}_1(-\bar{\eta})q_2(-\bar{\eta}),\\
\Phi_{02} =& f_{200000}\bar{q}_1^2(0) + f_{020000}\bar{q}_2^2(0) + f_{000200}\bar{q}_1^2(-\bar{\eta}) + 2f_{110000}\bar{q}_1(0)\bar{q}_2(0) + 2f_{101000}\bar{q}_1(0)\bar{q}_1(-1)\\
&+ 2f_{010100}\bar{q}_2(0)\bar{q}_1(-\bar{\eta}) + 2f_{010010}\bar{q}_2(0)\bar{q}_2(-\bar{\eta}) + 2f_{000110}\bar{q}_1(-\bar{\eta})\bar{q}_2(-\bar{\eta}),\\
\Phi_{30} =& f_{300000}q_1^3(0) + f_{030000}q_2^3(0) + f_{000300}q_1^3(-\bar{\eta}) + 3f_{210000}q_1^2(0)q_2(0) + 3f_{000210}q_1^2(-\bar{\eta})q_2(-\bar{\eta})\\
&+ 3f_{120000}q_1(0)q_2^2(0) + 3f_{010200}q_2(0)q_1^2(-\bar{\eta}) + 6f_{010110}q_2(0)q_1(-\bar{\eta})q_2(-\bar{\eta}),\\
\Phi_{03} =& f_{300000}\bar{q}_1^3(0) + f_{030000}\bar{q}_2^3(0) + f_{000300}\bar{q}_1^3(-\bar{\eta}) + 3f_{210000}\bar{q}_1^2(0)\bar{q}_2(0) + 3f_{000210}\bar{q}_1^2(-\bar{\eta})\bar{q}_2(-\bar{\eta})\\
&+ 3f_{120000}\bar{q}_1(0)\bar{q}_2^2(0) + 3f_{010200}\bar{q}_2(0)\bar{q}_1^2(-\bar{\eta}) + 6f_{010110}\bar{q}_2(0)\bar{q}_1(-\bar{\eta})\bar{q}_2(-\bar{\eta}),\\
\Phi_{21} =& 3f_{300000}q_1^2(0)\bar{q}_1(0) + 3f_{030000}q_2^2(0)\bar{q}_2(0) + 3f_{000300}q_1^2(-\bar{\eta})\bar{q}_1(-\bar{\eta})\\
&+ 3f_{210000}\left(q_1^2(0)\bar{q}_2(0) + 2q_1(0)q_2(0)\bar{q}_1(0)\right) + 3f_{000210}\left(q_1^2(-\bar{\eta})\bar{q}_2(-\bar{\eta}) + 2q_1(-\bar{\eta})q_2(-\bar{\eta})\bar{q}_1(-\bar{\eta})\right)\\
&+ 3f_{120000}\left(\bar{q}_1(0)q_2^2(0) + 2q_2(0)\bar{q}_2(0)q_1(0)\right) + 3f_{010200}\left(q_1^2(-\bar{\eta})\bar{q}_2(0) + 2q_1(-\bar{\eta})q_2(0)\bar{q}_1(-\bar{\eta})\right)\\
&+ 6f_{010110}\left(q_2(0)q_1(-\bar{\eta})\bar{q}_2(-\bar{\eta}) + q_2(0)q_2(-\bar{\eta})\bar{q}_1(-\bar{\eta}) + \bar{q}_2(0)q_1(-\bar{\eta})q_2(-\bar{\eta})\right),\\
\Phi_{12} =& 3f_{300000}\bar{q}_1^2(0)q_1(0) + 3f_{030000}\bar{q}_2^2(0)q_2(0) + 3f_{000300}\bar{q}_1^2(-\bar{\eta})q_1(-\bar{\eta})\\
&+ 3f_{210000}\left(\bar{q}_1^2(0)q_2(0) + 2q_1(0)\bar{q}_2(0)\bar{q}_1(0)\right) + 3f_{000210}\left(\bar{q}_1^2(-\bar{\eta})q_2(-\bar{\eta}) + 2q_1(-\bar{\eta})\bar{q}_2(-\bar{\eta})\bar{q}_1(-\bar{\eta})\right)\\
&+ 3f_{120000}\left(q_1(0)\bar{q}_2^2(0) + 2q_2(0)\bar{q}_2(0)\bar{q}_1(0)\right) + 3f_{010200}\left(\bar{q}_1^2(-\bar{\eta})q_2(0) + 2q_1(-\bar{\eta})\bar{q}_2(0)\bar{q}_1(-\bar{\eta})\right)\\
&+ 6f_{010110}\left(q_2(0)\bar{q}_1(-\bar{\eta})\bar{q}_2(-\bar{\eta}) + \bar{q}_2(0)\bar{q}_2(-\bar{\eta})q_1(-\bar{\eta}) + \bar{q}_2(0)\bar{q}_1(-\bar{\eta})q_2(-\bar{\eta})\right).
\end{aligned}$$

Denote

$$\begin{aligned}
\varphi(\kappa) + z(\kappa) =& \mathcal{Q}(\kappa)m_x + z(\kappa) = q(\kappa)m_1(t)b_{n_s}(x) + \bar{q}(\kappa)m_2(t)b_{n_s}(x) + z(\kappa)\\
=& \begin{pmatrix} q_1(\kappa)m_1(t)b_{n_s}(x) + \bar{q}_1(\kappa)m_2(t)b_{n_s}(x) + z_1(\kappa)\\ q_2(\kappa)m_1(t)b_{n_s}(x) + \bar{q}_2(\kappa)m_2(t)b_{n_s}(x) + z_2(\kappa)\end{pmatrix} = \begin{pmatrix}\varphi_1(\kappa) + z_1(\kappa)\\ \varphi_2(\kappa) + z_2(\kappa)\end{pmatrix}.
\end{aligned} \tag{B.5}$$

Similarly, we have

$$F_2(\mathcal{Q}(\kappa)m_x + z, 0) = \sum_{u_1+u_2=2}\Phi_{u_1u_2}m_1^{u_1}m_2^{u_2}b_{n_s}^2(x) + \mathcal{S}_2(\mathcal{Q}(\kappa)m_x, z) + O\left(|z|^2\right),\ u_1, u_2 \in \mathrm{N}_0. \tag{B.6}$$

Combining Eqs (B.1), (B.5) and (B.6), we have

$$\begin{aligned}
\mathcal{S}_2(\mathcal{Q}(\kappa)m_x, z) =& [2f_{200000}q_1(0)z_1(0) + 2f_{020000}q_2(0)z_2(0) + 2f_{000200}q_1(-\bar{\eta})z_1(-\bar{\eta})\\
&+ 2f_{110000}(q_1(0)z_2(0) + q_2(0)z_1(0)) + 2f_{101000}(q_1(0)z_1(-1) + q_1(-1)z_1(0))\\
&+ 2f_{010100}(q_2(0)z_1(-\bar{\eta}) + q_1(-\bar{\eta})z_2(0)) + 2f_{010010}(q_2(0)z_2(-\bar{\eta}) + q_2(-\bar{\eta})z_2(0))\\
&+ 2f_{000110}(q_1(-\bar{\eta})z_2(-\bar{\eta}) + q_2(-\bar{\eta})z_1(-\bar{\eta}))]m_1(t)b_n(x)
\end{aligned}$$

$$
\begin{aligned}
&+ [2f_{200000}\bar{q}_1(0)z_1(0) + 2f_{020000}\bar{q}_2(0)z_2(0) + 2f_{000200}\bar{q}_1(-\bar{\eta})z_1(-\bar{\eta})\\
&+ 2f_{110000}(\bar{q}_1(0)z_2(0) + \bar{q}_2(0)z_1(0)) + 2f_{101000}(\bar{q}_1(0)z_1(-1) + \bar{q}_1(-1)z_1(0))\\
&+ 2f_{010100}(\bar{q}_2(0)z_1(-\bar{\eta}) + \bar{q}_1(-\bar{\eta})z_2(0)) + 2f_{010010}(\bar{q}_2(0)z_2(-\bar{\eta}) + \bar{q}_2(-\bar{\eta})z_2(0))\\
&+ 2f_{000110}(\bar{q}_1(-\bar{\eta})z_2(-\bar{\eta}) + \bar{q}_2(-\bar{\eta})z_1(-\bar{\eta}))]m_2(t)b_n(x).
\end{aligned}
$$

**The calculations of $h_{0,11}(\kappa)$, $h_{0,20}(\kappa)$, $h_{2n_s,11}(\kappa)$ and $h_{2n_s,20}(\kappa)$**

From [44], there is

$$
M_2^2\left(h_n(\kappa,m)b_n(x)\right) = \mathcal{D}_m\left(h_n(\kappa,m)b_n(x)\right)\mathcal{V}m - \mathcal{A}_{\mathcal{P}^1}\left(h_n(\kappa,m)b_n(x)\right),
$$

which causes

$$
\begin{aligned}
\left(\begin{bmatrix} M_2^2\left(h_n(\kappa,m)b_n(x)\right), \beta_n^{(1)} \\ M_2^2\left(h_n(\kappa,m)b_n(x)\right), \beta_n^{(2)} \end{bmatrix}\right) =& 2i\omega\tau^*\left(h_{n,20}(\kappa)m_1^2 - h_{n,02}(\kappa)m_2^2\right)\\
&- \left(\dot{h}_n(\kappa,m) + Z_0(\kappa)\left(\mathcal{L}_0\left(h_n(\kappa,m)\right) - \dot{h}_n(0,m)\right)\right),
\end{aligned}
\tag{B.7}
$$

where

$$
\mathcal{L}_0\left(h_n(\kappa,m)\right) = -\tau^*(\frac{n}{l})^2 B_1 h_n(0,m) + \tau^*\left(A_1 h_n(0,m) + A_2 h_n(-1,m) + A_3 h_n(-\bar{\eta},m)\right).
$$

By combining (A.8) with the second equation of (A.13), we have

$$
\begin{aligned}
f_2^2(m,0,0) =& Z_0(\kappa)\tilde{F}_2(Q(\kappa)m_x,0) - \pi\left(Z_0(\kappa)\tilde{F}_2(Q(\kappa)m_x,0)\right)\\
=& Z_0(\kappa)\tilde{F}_2(Q(\kappa)m_x,0) - Q(\kappa)\mathcal{P}(0)\left(\begin{bmatrix} \tilde{F}_2(Q(\kappa)m_x,\ 0),\ \beta_{n_s}^{(1)} \\ \tilde{F}_2(Q(\kappa)m_x,\ 0),\ \beta_{n_s}^{(2)} \end{bmatrix}\right) b_{n_s}(x).
\end{aligned}
\tag{B.8}
$$

From Eqs (A.32), (A.33) and (A.34), we have

$$
\left(\begin{bmatrix} f_2^2(m,0,0),\beta_n^{(1)} \\ f_2^2(m,0,0),\beta_n^{(2)} \end{bmatrix}\right) = \begin{cases} \dfrac{1}{\sqrt{l\pi}}Z_0(\kappa)\left(\Phi_{20}m_1^2 + \Phi_{02}m_2^2 + \Phi_{11}m_1m_2\right),\ n=0, \\ \dfrac{1}{\sqrt{2l\pi}}Z_0(\kappa)\left(\tilde{\Phi}_{20}m_1^2 + \tilde{\Phi}_{02}m_2^2 + \tilde{\Phi}_{11}m_1m_2\right),\ n=2n_s, \end{cases}
\tag{B.9}
$$

where $\tilde{\Phi}_{ij}$ is represented by the following equation

$$
\begin{cases} \tilde{\Phi}_{ij} = \Phi_{ij} - 2(\dfrac{n_s}{l})^2\Phi_{ij}^d, \\ i,j = 0,1,2,\ i+j=2, \end{cases}
\tag{B.10}
$$

and the expression for $\Phi_{ij}^d$ is given by (A.35). Therefore, by combining (B.7)–(B.9) and matching coefficients of $m_1^2$, $m_1m_2$, we obtain

$$
n=0,\begin{cases} m_1^2 : \begin{cases} \dot{h}_{0,20}(\kappa) - 2i\omega\tau^* h_{0,20}(\kappa) = (0,0)^T, \\ \dot{h}_{0,20}(0) - L_0(h_{0,20}(\kappa)) = \dfrac{1}{\sqrt{l\pi}}\Phi_{20}, \end{cases} \\ m_1m_2 : \begin{cases} \dot{h}_{0,11}(\kappa) = (0,0)^T, \\ \dot{h}_{0,11}(0) - L_0(h_{0,11}(\kappa)) = \dfrac{1}{\sqrt{l\pi}}\Phi_{11}, \end{cases} \end{cases}
\tag{B.11}
$$

$$n = 2n_s, \begin{cases} m_1^2 : \begin{cases} \dot{h}_{2n_s,20}(\kappa) - 2i\omega\tau^* h_{2n_s,20}(\kappa) = (0,0)^T, \\ \dot{h}_{2n_s,20}(0) - \mathcal{L}_0(h_{2n_s,20}(\kappa)) = \dfrac{1}{\sqrt{2l\pi}}\tilde{\Phi}_{20}, \end{cases} \\ m_1 m_2 : \begin{cases} \dot{h}_{2n_s,11}(\kappa) = (0,0)^T, \\ \dot{h}_{2n_s,11}(0) - \mathcal{L}_0(h_{2n_s,11}(\kappa)) = \dfrac{1}{\sqrt{2l\pi}}\tilde{\Phi}_{11}. \end{cases} \end{cases} \tag{B.12}$$

By solving Eqs (B.11) and (B.12), we obtain the following results

$$\begin{aligned} h_{0,20}(\kappa) =& \frac{1}{\sqrt{l\pi}} e^{2i\omega\tau^*\kappa} \left(2i\omega\tau^* I_2 - \tau^* A_1 - \tau^* A_2 e^{-2i\omega\tau^*} - \tau^* A_3 e^{-2i\omega\tau_2}\right)^{-1} \Phi_{20}, \\ h_{0,11}(\kappa) =& \frac{1}{\sqrt{l\pi}} \left(-\tau^* A_1 - \tau^* A_2 - \tau^* A_3\right)^{-1} \Phi_{11}, \\ h_{2n_s,20}(\kappa) =& \frac{1}{\sqrt{2l\pi}} e^{2i\omega\tau^*\kappa} \left(2i\omega\tau^* I_2 + \tau^*(\frac{2n_s}{l})^2 B_1 - \tau^* A_1 - \tau^* A_2 e^{-2i\omega\tau^*} - \tau^* A_3 e^{-2i\omega\tau_2}\right)^{-1} \tilde{\Phi}_{20}, \\ h_{2n_s,11}(\kappa) =& \frac{1}{\sqrt{2l\pi}} \left(\tau^*(\frac{2n_s}{l})^2 B_1 - \tau^* A_1 - \tau^* A_2 - \tau^* A_3\right)^{-1} \tilde{\Phi}_{11}. \end{aligned}$$

## Use of AI tools declaration

The authors declare they have not used Artificial Intelligence (AI) tools in the creation of this article.


## Acknowledgments

This work is supported by the National Natural Science Foundation of China (12171135, 11771115), the Research Funding for High-Level Innovative Talents of Hebei University (801260201242).


## Conflict of interest

The authors declare there are no conflicts of interest.

## References


1. F. M. Alwan, D. K. Archana, D. G. Prakasha, H. A. Ali, Computational optimization of fractional-order influenza sir epidemic modeling using two effective techniques, *Commun. Math. Biol. Neurosci.*, **2025** (2025), 101. https://doi.org/10.28919/cmbn/9401
2. Y. Javaid, S. Jawad, R. Ahmed, H. A. Ali, B. Rashwani, Dynamic complexity of a discretized predator prey system with allee effect and herd behaviour, *Appl. Math. Sci. Eng.*, **32** (2024), 2420953. https://doi.org/10.1080/27690911.2024.2420953
3. H. A. Ali, A. Ahmad, F. Abbas, E. Hincal, A. Ghaffar, B. Batiha, et al., Modeling the behavior of a generalized cholera epidemic model with asymptomatic measures for early detection, *PLoS One*, **20** (2025), e0319684. https://doi.org/10.1371/journal.pone.0319684

4. A. Ali, S. Jawad, Stability analysis of the depletion of dissolved oxygen for the phytoplankton-zooplankton model in an aquatic environment, *Iraqi J. Sci.*, **65** (2024), 2736–2748. https://doi.org/10.24996/ijs.2024.65.5.31
5. A. Lotka, *Elements of Physical Biology*, Williams and Wilkins, Baltimore, 1925. https://doi.org/10.1038/116461b0
6. V. Volterra, Fluctuations in the abundance of a species considered mathematically, *Nature*, **118** (1926), 558–560. https://doi.org/10.1038/118558a0
7. H. I. Freedman, P. Waltman, Persistence in models of three interacting predator-prey populations, *Math. Biosci.*, **68** (1984), 213–231. https://doi.org/10.1016/0025-5564(84)90032-4
8. P. Y. H. Pang, M. Wang, Strategy and stationary pattern in a three-species predator-prey model, *J. Differ. Equations*, **200** (2004), 245–273. https://doi.org/10.1016/j.jde.2004.01.004
9. M. Wang, P. Y. H. Pang, Global asymptotic stability of positive steady states of a diffusive ratio-dependent prey-predator model, *Appl. Math. Lett.*, **21** (2008), 1215–1220. https://doi.org/10.1016/j.aml.2007.10.026
10. X. Tang, Y. Song, Cross-diffusion induced spatiotemporal patterns in a predator-prey model with herd behavior, *Nonlinear Anal. Real World Appl.*, **24** (2015), 36–49. https://doi.org/10.1016/j.nonrwa.2014.12.006
11. D. Wu, H. Zhao, Spatiotemporal dynamics of a diffusive predator-prey system with Allee effect and threshold hunting, *J. Nonlinear Sci.*, **30** (2020), 1015–1054. https://doi.org/10.1007/s00332-019-09600-0
12. D. Sen, S. Ghorai, M. Banerjee, A. Morozov, Bifurcation analysis of the predator-prey model with the Allee effect in the predator, *J. Math. Biol.*, **84** (2022), 7. https://doi.org/10.1007/s00285-021-01707-x
13. C. Wang, S. Yuan, H. Wang, Spatiotemporal patterns of a diffusive prey-predator model with spatial memory and pregnancy period in an intimidatory environment, *J. Math. Biol.*, **84** (2022), 12. https://doi.org/10.1007/s00285-022-01716-4
14. C. S. Holling, Some characteristics of simple types of predation and parasitism, *Can. Entomol.* **91** (1959), 385–398. https://doi.org/10.4039/Ent91385-7
15. J. Zhou, Positive steady state solutions of a Leslie-Gower predator-prey model with Holling type II functional response and density-dependent diffusion, *Nonlinear Anal. Theory Methods Appl.*, **82** (2013), 47–65. https://doi.org/10.1016/j.na.2012.12.014
16. N. Ali, M. Jazar, Global dynamics of a modified Leslie-Gower predator-prey model with Crowley-Martin functional responses, *J. Appl. Math. Comput.*, **43** (2013), 271–293. https://doi.org/10.1007/s12190-013-0663-3
17. P. Lenzini, J. Rebaza, Nonconstant predator harvesting on ratio-dependent predator-prey models, *Appl. Math. Sci.*, **4** (2010), 791–803.
18. H. Shi, W. Li, G. Lin, Positive steady states of a diffusive predator-prey system with modified Holling-Tanner functional response, *Nonlinear Anal. Real World Appl.*, **11** (2010), 3711–3721. https://doi.org/10.1016/j.nonrwa.2010.02.001

19. X. Chen, Z. Du, Existence of positive periodic solutions for a neutral delay predator-prey model with Hassell-Varley type functional response and impulse, *Qual. Theory Dyn. Syst.*, **17** (2018), 67–80. https://doi.org/10.1007/s12346-017-0223-6

20. Y. Li, S. Huang, T. Zhang, Dynamics of a non-selective harvesting predator-prey model with Hassell-Varley type functional response and impulsive effects, *Math. Methods Appl. Sci.*, **39** (2016), 189–201. https://doi.org/10.1002/mma.3468

21. Y. Zhang, J. Huang, Bifurcation analysis of a predator-prey model with beddington-deangelis functional response and predator competition, *Math. Methods Appl. Sci.*, **45** (2022), 9894–9927. https://doi.org/10.1002/mma.8345

22. D. Luo, The study of global stability of a periodic Beddington-DeAngelis and Tanner predator-prey model, *Results Math.*, **74** (2019), 101. https://doi.org/10.1007/s00025-019-1016-9

23. A. Singh, P. Malik, Bifurcations in a modified Leslie-Gower predator-prey discrete model with Michaelis-Menten prey harvesting, *J. Appl. Math. Comput.*, **67** (2021), 143–174. https://doi.org/10.1007/s12190-020-01491-9

24. R. Yang, C. Zhang, Dynamics in a diffusive predator-prey system with a constant prey refuge and delay, *Nonlinear Anal. Real World Appl.*, **31** (2016), 1–22. https://doi.org/10.1016/j.nonrwa.2016.01.005

25. W. Yang, Global asymptotical stability and persistent property for a diffusive predator-prey system with modified Leslie-Gower functional response, *Nonlinear Anal. Real World Appl.*, **14** (2013), 1323–1330. https://doi.org/10.1016/j.nonrwa.2012.09.020

26. R. Yang, Bifurcation analysis of a diffusive predator-prey system with Crowley-Martin functional response and delay, *Chaos, Solitons Fractals*, **95** (2017), 131–139. https://doi.org/10.1016/j.chaos.2016.12.014

27. X. Zhang, H. Zhu, Q. An, Dynamics analysis of a diffusive predator-prey model with spatial memory and nonlocal fear effect, *J. Math. Anal. Appl.*, **525** (2023), 127123. https://doi.org/10.1016/j.jmaa.2023.127123

28. X. Tao, L. Zhu, Study of periodic diffusion and time delay induced spatiotemporal patterns in a predator-prey system, *Chaos, Solitons Fractals*, **150** (2021), 111101. https://doi.org/10.1016/j.chaos.2021.111101

29. F. Liu, R. Yang, L. Tang, Hopf bifurcation in a diffusive predator-prey model with competitive interference, *Chaos, Solitons Fractals*, **120** (2019), 250–258. https://doi.org/10.1016/j.chaos.2019.01.029

30. Y. Lou, W. Ni, Diffusion, self-diffusion and cross-diffusion, *J. Differ. Equations*, **131** (1996), 79–131. https://doi.org/10.1006/jdeq.1996.0157

31. W. Zuo, Global stability and Hopf bifurcations of a Beddington-DeAngelis type predator-prey system with diffusion and delays, *Appl. Math. Comput.*, **223** (2013), 423–435. https://doi.org/10.1016/j.amc.2013.08.029

32. J. Cao, H. Sun, P. Hao, P. Wang, Bifurcation and turing instability for a predator-prey model with nonlinear reaction cross-diffusion, *Appl. Math. Modell.*, **89** (2021), 1663–1677. https://doi.org/10.1016/j.apm.2020.08.030

33. X. Lin, H. Wang, Stability analysis of delay differential equations with two discrete delays, *Can. Appl. Math. Q.*, **20** (2012), 519–533.
34. J. Cao, L. Ma, P. Hao, Bifurcation analysis in a modified Leslie-Gower predator-prey model with Beddington-DeAngelis functional response, *J. Appl. Anal. Comput.*, **13** (2023), 3026–3053. https://doi.org/10.11948/20230183
35. S. Li, S. Yuan, Z. Jin, H. Wang, Bifurcation analysis in a diffusive predator-prey model with spatial memory of prey, Allee effect and maturation delay of predator, *J. Differ. Equations*, **357** (2023), 32–63. https://doi.org/10.1016/j.jde.2023.02.009
36. H. Sun, J. Cao, P. Hao, L. Zhang, Instability and bifurcation analysis of a diffusive predator-prey model with fear effect and delay, *Int. J. Biomath.*, **17** (2024), 2350080. https://doi.org/10.1142/S1793524523500808
37. H. Sun, P. Hao, J. Cao, Dynamics analysis of a diffusive prey-taxis system with memory and maturation delays, *Electron. J. Qual. Theory Differ. Equations*, **40** (2024), 1–20. https://doi.org/10.14232/ejqtde.2024.1.40
38. J. Liu, J. Chen, C. Tian, Stability of Turing bifurcation in a weighted networked reaction-diffusion system, *Appl. Math. Lett.*, **118** (2021), 107135. https://doi.org/10.1016/j.aml.2021.107135
39. J. K. Hale, *Theory of Functional Differential Equations*, Springer-Verlag, New York, 1977. https://doi.org/10.1007/978-1-4612-9892-2
40. Y. Du, B. Niu, J. Wei, Two delays induce Hopf bifurcation and double Hopf bifurcation in a diffusive Leslie-Gower predator-prey system, *Chaos*, **29** (2019), 013101. https://doi.org/10.1063/1.5078814
41. Y. Song, Y. Peng, T. Zhang, The spatially inhomogeneous Hopf bifurcation induced by memory delay in a memory-based diffusion system, *J. Differ. Equations*, **300** (2021), 597–624. https://doi.org/10.1016/j.jde.2021.08.010
42. Y. Lv, The spatially homogeneous Hopf bifurcation induced jointly by memory and general delays in a diffusive system, *Chaos, Solitons Fractals*, **156** (2022), 111826. https://doi.org/10.1016/j.chaos.2022.111826
43. S. N. Chow, J. K. Hale, *Methods of Bifurcation Theory*, Springer-Verlag, New York, 1982. https://doi.org/10.1007/978-1-4613-8159-4
44. T. Faria, Normal forms and Hopf bifurcation for partial differential equations with delays, *Trans. Amer. Math. Soc.*, **352** (2000), 2217–2238. https://doi.org/10.1090/S0002-9947-00-02280-7



AIMS Press

© 2025 the Author(s), licensee AIMS Press. This is an open access article distributed under the terms of the Creative Commons Attribution License (https://creativecommons.org/licenses/by/4.0)